Kollsman Instrument Corporation

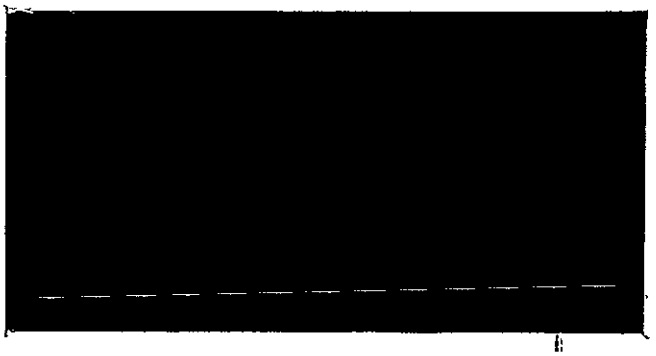

ACCESSION NO.	PRICE	COPIES REQUIRED	DATE REQUESTED	REQUEST NO.
N65-13138				
COVER COLOR	NO. OF PAGES		DATE DUE	DATE RECEIVED

TITLE

PLATES	QUANTITY	COST	PRESS	QUANTITY	COST
XEROX			BINDERY		
ITEK			IMPRESSIONS		
OTHER			NUMBER OF SHEETS		
TOTALS			**TOTALS**		
RECEIVED	R & P	WAREHOUSE	INVENTORY		

REMARKS

1 Copy
CFSTI
XEROX - 2400
4-1-69

FORM NBS-805
(10-26-64)

U.S. DEPARTMENT OF COMMERCE
NATIONAL BUREAU OF STANDARDS

CLEARINGHOUSE PRINTING REQUEST

kollsman instrument corporation

Copy No. 13

KOLLSMAN INSTRUMENT CORPORATION
80-08 45th Avenue
Elmhurst, New York 11373

Bi-Monthly Technical Report
NASA Contract No. NASW-929

15 October 1964

KIC-RD-000162-1

STUDY OF LASER POINTING PROBLEMS

Prepared For
NATIONAL AERONAUTICS AND SPACE ADMINISTRATION
Washington, D. C. 20546

CORPORATE TECHNOLOGY CENTER
KOLLSMAN INSTRUMENT CORPORATION

STUDY OF LASER POINTING PROBLEMS

Kollsman Instrument Corporation
Elmhurst, NY

Oct 64

KOLLSMAN INSTRUMENT CORPORATION
CORPORATE TECHNOLOGY CENTER
80-08 45TH AVENUE
ELMHURST, NEW YORK 11373

BI-MONTHLY TECHNICAL REPORT
NO. KIC-RD-000162-1

STUDY OF LASER POINTING PROBLEMS

Report Period: 3 August 1964-30 September 1964

NASA Contract No. NASW-929

Prepared for
NATIONAL AERONAUTICS AND SPACE ADMINISTRATION
Washington, D. C. 20546

Prepared By:

Aaron Wallace
Aaron Wallace
Project Director

Approved:

Nathan Kaplan
Dr. Nathan Kaplan
Director of Center

FOREWORD

This Bi-Monthly Technical Report, entitled "Study of Laser Pointing Problems". was prepared in accordance with NASA Contract No. NSAW-929, Article IV B. This first technical report covers the period 3 August-30 September 1964. The work is carried out under the direction of Mr. R. F. Bohling, NASA Headquarters, and Mr. F. R. Morrell, NASA, Langley Research Center. The studies described herein were performed by Aaron Wallace, Project Director, Roger Arguello, Dr. Sebastian Monaco, John Meader and Judah Eichenthal of the Corporate Technology Center, Systems and Space Division staffs of the Kollsman Instrument Corporation.

ABSTRACT

The remarkable potential of deep space laser communications based on low power transmitters in deep space vehicles, extremely narrow beamwidths (0.01-1.0 arc seconds), and very wide-band frequency channels can be fully exploited only when the laser beam pointing problem is solved. Of particular interest is the mission of communication from a deep space vehicle directly to Earth.

This first Bi-Monthly Technical Report describes the progress made in the major technical areas of systems analysis and synthesis, establishment of reference axes, techniques for measuring and positioning the laser beam, and boresight maintenance. The presence of the Earth's atmosphere in the communication link with its random turbulence phenomena profoundly affects the system design, and introduces additional requirements for system synthesis beyond those associated with the extraordinary optical precision due to the narrow beamwidths and the dynamics of closed loop operation with transit time effects and target-observer motions.

The report also includes manpower utilization data and concludes with a bibliography of cited references.

TABLE OF CONTENTS

TABLE OF CONTENTS
(Cont'd.)

LIST OF ILLUSTRATIONS

LIST OF ILLUSTRATIONS
(Cont'd.)

LIST OF TABLES

I. INTRODUCTION

The United States Aerospace investigation and exploration programs under the direction of NASA include families of lunar and near interplanetary missions, far interplanetary and interstellar probes, observatory satellites, and numerous scientific satellites, Refs.(1), (2). From a scientific point of view, the amount of information and data to be generated in the course of these missions is expected to be enormous, as well as of the highest importance for this nation's continued progress in science and space exploration.

It is evident that the successful implementation of these programs will depend upon progress in the propulsion and communication fields. Although a considerable number of advances have already taken place in these areas, it is clear that new communications channels must be developed since the present-day booster-rocket and microwave communications technologies are already approaching ideal performance limitations, Refs. (1),(2),(3). Optical communications based on the current rapidly expanding laser technology may provide the necessary breakthrough because of the unprecedented space and frequency bandwidths made available as a result of the laser's spatial and temporal coherence, Refs. (4), (5).

However, the remarkable potential of deep space laser communications based on low power transmitters, extremely narrow beamwidths, and very wideband frequency channels involving high data transmission rates cannot be fully exploited unless the laser beam pointing problem is solved, Ref. (2), p.63, Ref. (3), p.64, Ref. (6). The Kollsman Instrument Corporation is already deeply involved in optical tracking systems for NASA and the Air Force, i.e., the Apollo optical guidance, the OAO star tracker attitude stabilization, OAO pointing control, the Goddard Experiment Package for the OAO, and celestial-inertial guidance systems for the Air Force B-52, the B-58, the B-47, the Hound Dog, and the USQ-28 geodetic survey and photomapping system for Project "Sky Map", as well as many other similar programs. Consequently, some of the major problems associated with the Laser Beam Pointing System have been previously encountered in one form or another in connection with Kollsman's optical and stellar guidance programs. Technical problems uniquely associated with the laser and coherent light control

have also been previously met in connection with Kollsman projects involving laser airborne, ground, and underwater radars, laser alignment systems, laser metrological and metallurgical systems, etc.

Finally, Kollsman experience and research activities in the systems synthesis, system analysis, control, and computer fields have led to the conclusion that a systems approach to the Laser Beam Pointing Problem is required in addition to the application of specific technical knowledge to the detailed solution of its component aspects. This systems approach was originally described in Ref. (7), and the detailed program activities to implement this approach are outlined below. A detailed exposition of the basic elements of general systems philosophy is given in Ref. (8). Application of systems theory to this problem leads to the major conclusion that the presence of the Earth's atmosphere in the communication link with its random turbulence phenomena profoundly affects the system design. As a result, additional requirements for system synthesis are introduced beyond those associated with the extraordinary optical precision due to the narrow beamwidths and the dynamics of closed-loop operation with transit time effects and target-observer motion.

A. PROGRAM OBJECTIVES

The objective of this contract is to define the fundamental limitations, practical implementation problems, and research problems associated with the technology that will enable the use of 0.01-1.0 arc second laser beams for deep space communication with less than 3db degradation resulting from the pointing accuracy during operation.

The Contractor shall perform studies toward the above objective and shall give consideration to the following major problems among others:

(1) Techniques for detecting and establishing suitable references axes from which to derive pointing information for the laser beam.

(2) Techniques for measuring and positioning the optical pointing axis with respect to the reference axes and/or with respect to incident radiation from the desired cooperative second terminal.

(3) Techniques for maintaining boresight between the optical and mechanical axes of the laser.

References: (9), Art. III; (10), Attachment III, Art. III; (7), Sect. I, p.1.

It is specified that "when it becomes necessary or desirable to consider the second terminal in the communications link, that terminal shall be assumed to be on earth. This space-to-earth link has been selected since it entails problems which are representative, and also is the most likely system to receive early implementation. Where systems are used as guides to study acquisition and tracking problems, they should be considered cooperative communication links. Complexity of the ground installation is considered a secondary restraint on the communication link, and assumptions regarding the ground portion should be constrained only by technical and economic feasibility", Ref. (9), Art. IIIC, Guidelines.

B. PROGRAM TASKS AND SCHEDULES

1. Task Breakdown, Ref. (9), Art. III

Phase I - Problem Investigation - Five (5) Months

The Contractor will investigate all salient features of the problem as defined in "Objectives" above germane to pointing accuracy.

Phase II- Methods of Solution-Three and One-Half (3-1/2) Months

The Contractor shall examine the trade-offs involved between alternate solutions to the problem in light of the investigation performed in Phase I. The Contractor shall analyze each solution and determine those offering the greatest potential of success.

Phase III- Definition of Research Problems - One and One-Half (1-1/2) Months

The Contractor shall, on the basis of Phase I and Phase II, define areas in which basic and applied research is required in order that the objective, as defined in "Objectives", may be realized.

2. Detailed Task Breakdown

The following task numbers and descriptions are assigned for the duration of Phase I (five months). Phase II and Phase III assignments will be made upon Phase I completion. A flow chart of project activities is shown in Figure 1, and the information flow and schedule (including milestones, reviews, and reports) are given in Figure 2. However, it probably will be necessary to modify the individual task schedules as the program develops to allow for greater weighting of specific tasks as required.

Task No.	Description
01	Planning and Administration
02	Laser Communications Systems
03	General Beam Pointing System Analysis
04	One Arc Second System Analysis
05	Tenth Arc Second System Analysis
06	Hundredth Arc Second System Analysis
	(Tasks 04, 05, 06 generate Beam Pointing System Diagrams with first order assignment of system, optical, electromagnetic, inertial, kinematic, mechanical, and electronic transfer functions for first order error and trade-off system analysis).
10	Techniques for detecting and establishing suitable reference axes from which to derive pointing information for the laser beam - General Analysis.
11	Celestial Data - Reference frames, missions, background, sensors, - e.g., astronomical/terrestrial coordinates, attitude stabilization, orbital parameters, interplanetary media, stellar sources, electro-optical image sensors, star trackers, etc.
12	Inertial Data - Missions, kinematics, sensors, celestial interfaces, - e.g., orbital data, parameters, inertial and stellar-inertial systems, coordinate systems, attitude systems.
13	DSIF Data - Missions, measurements, telemetry, spacecraft sensors, - e.g., terrestrial-astronomical coordinates, data characteristics, readout, spacecraft and ground links, computer interfaces, cooperative interfaces.

- Cont'd -

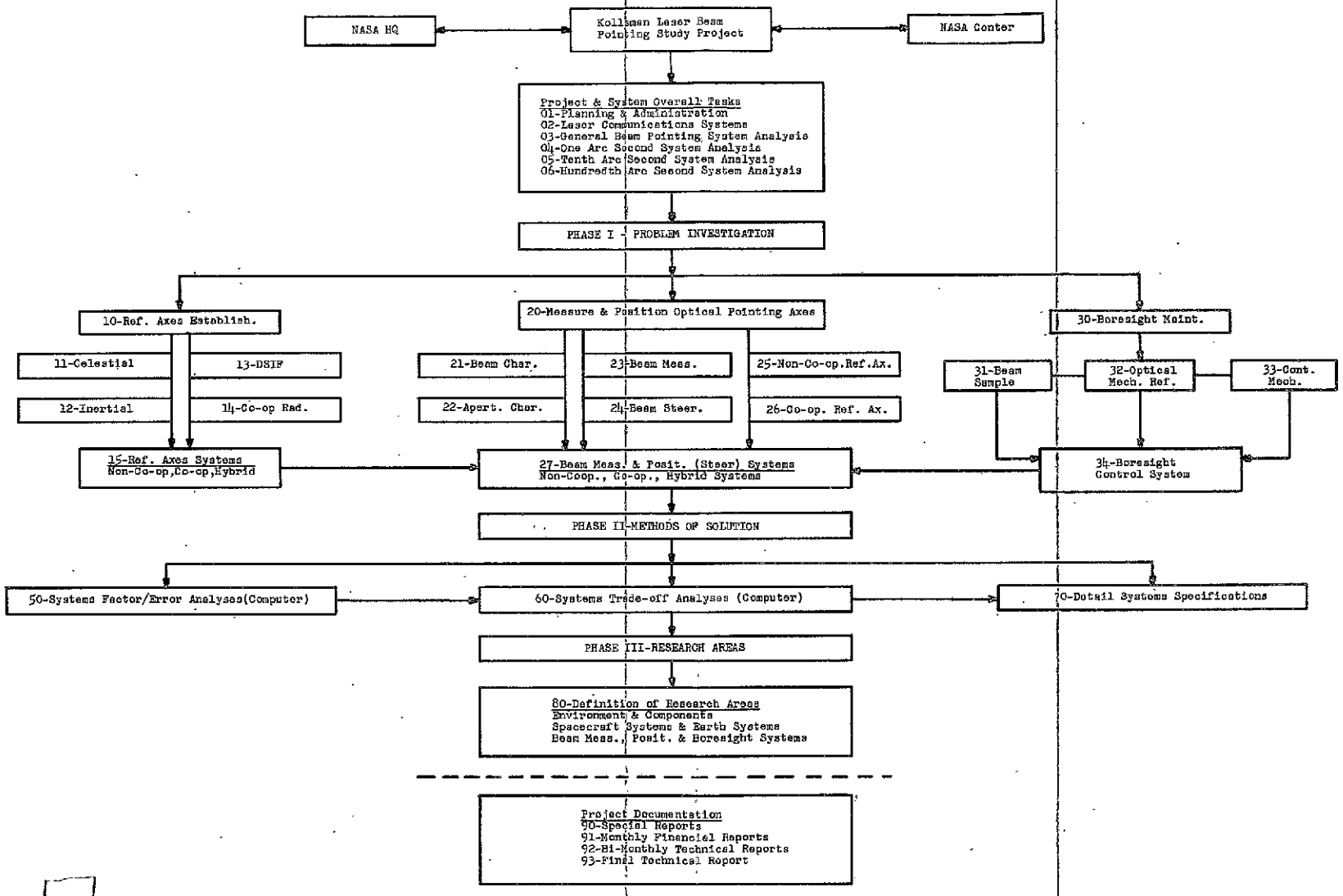

Figure 1. Laser Beam Pointing Study Project Activities

A

B

5a

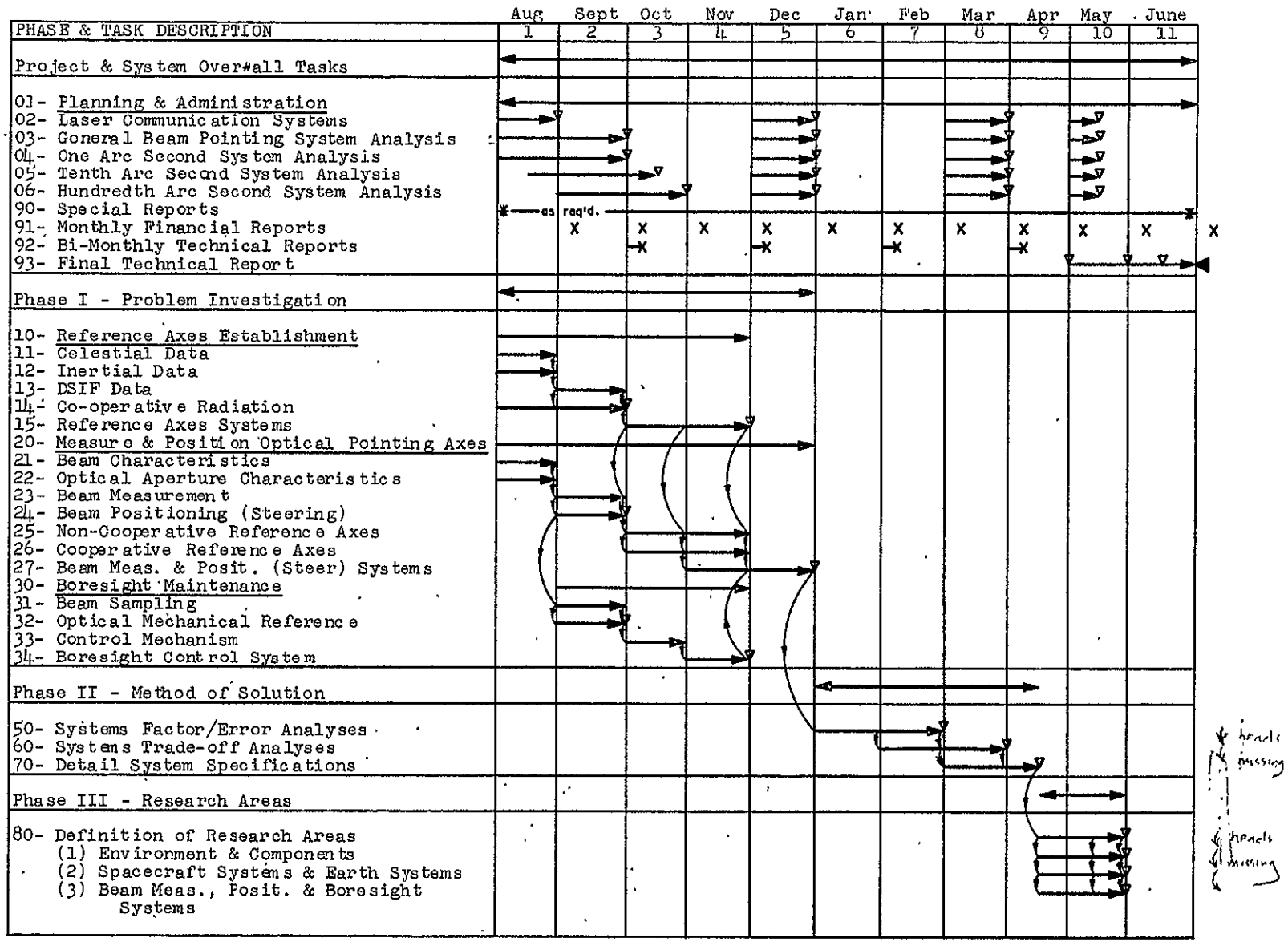

Notes: (1) Phase I - 5 months; Phase II - 3-1/2 months; Phase III - 1-1/2 months.
(2) Bi-Monthly Reports are due on 15th day following every second month (—✕).
(3) Final Technical Report is due on 30 June 1965, (◀).
(4) (▽) = Project Milestone Review.
(5) Special Reports will be prepared as required (*).

Figure 2. Laser Beam Pointing Study Project Schedules

Task No. (Cont'd)	Description
14	Cooperative Laser Radiation - Earth transmission and modulation, space reception and demodulation - e.g., acquisition, track, and communication modes, logic and control parameters, spacecraft and ground links, attitude control.
15	Reference Axes Systems - Non-cooperative, cooperative, and hybrid (combination non-cooperative and cooperative) - e.g., functional elements of combined systems derived from basic systems of 10-14 above, and physical implementation characteristics thereof, and study of major error sources (cf.03-06).
20	Techniques for measuring and positioning the optical pointing axes with respect to the reference axes and/or with respect to incident radiation from the desired cooperative second terminal (assumed to be on earth) - General Analysis.
21	Laser Beam Characteristics - Optical pointing axis, spatial, frequency, temporal, and intensity characteristics, relationships to Reference Axis Systems Functional Characteristics (02-06-15) above.
22	Optical Aperture Characteristics - Dimensions, parameters, control, stability, mechanical aspects of visibility, inertial balancing, reaction torques, combined systems for pointing and communications.
23	Laser Beam Measurement - Axis pickoffs, sensors, readouts, reference axis readouts, comparison circuits, relationships to systems characteristics.
24	Laser Beam Positioning and Steering - Control mechanisms, signals, electro-optical and mechanical components, counterbalancing, symmetrical inertial balancing, reaction torques.
25	Non-Cooperative Reference Axes - Interfaces with non-cooperative techniques developed in (10-15) above, specifically (11,12,13).
26	Cooperative Reference Axes - Interfaces with cooperative techniques developed in (10-15) above, specifically (13,14).

- Cont'd -

Task No. (Cont'd)	Description
27	Laser Beam Measuring and Positioning (Steering) Systems - Synthesis of three types of systems: non-cooperative, cooperative, and hybrid in terms of missions, subsystems, etc., based on the activities of tasks (02-06), (10,15), (20-26), and (30-34) below.
30	Techniques for Maintaining Boresight between the optical and mechanical axes of the Laser-General Analysis.
31	Laser Beam Sampling - Based on information generated in (21,22,23), above.
32	Optical Mechanical Reference - Interferometric and/or optical correlation elements mounted to laser mechanical axis structure for optical axis alignment comparison.
33	Control Mechanism - Feedback loops and circuits for operating on error signals derived from (31) and (32).
34	Boresight Control System - Synthesis of complete boresight maintenance systems based on design elements developed in (30-33), (02-06), (10,15), (20-26).

The following task numbers are assigned to cover "reporting requirements", i.e., "Deliverable Items" above, plus special reports as required, Reference (1), Art. IV A, B, C, D. These numbers are assigned for the Contract duration.

90	Special Reports for presentations and papers.
91	Monthly Financial Reports.
92	Bi-Monthly Technical Reports.
93	Final Technical Report

The following task number assignments are tentatively made for Phases II and III in order to reserve the serial number blocks so that continuity with the Phase I number sequence is maintained.

Phase II Task Numbers (Tentative)

50 Factor and Error Analysis of Systems generated in Phase I, Tasks (02-06), (15), (27), (34) to set the stage for the following trade-off analyses (see below). Computer simulation and computer error analysis will be employed.

60 Trade-off Analyses on the alternate solutions generated in Phase I, and analyzed in detail in the preceding task (50). These analyses will determine the systems offering the greatest potential of success. Computer simulation and trade-off analysis will be employed.

70 Detailed System Specification for the Systems Selected in the preceding task (60), namely, those with the greatest potential. This task will exhibit the characteristics of all system aspects and component elements which are presently available only as experimental devices, or else exist only in a theoretical sense, or else are beyond the present state of the art.

Phase III Task Numbers (Tentative)

80 Definition of Areas in which basic and applied research is required based on the results of Phases I and II, particularly task(s) (70), probably in the following categories:

(1) Environment and Components.
(2) Spacecraft systems and Earth systems.
(3) Laser Beam Measurement, Positioning, and Boresight Systems, etc.

PROJECT ACTIVITIES FLOW DIAGRAM AND TIME SCHEDULE

The preceding figures present the flow chart of project activities (Figure 1) and the information flow and time schedule (Figure 2). Since the accuracies specified for the Laser Beam Pointing Systems (1.0-0.01 arc second) are at the frontier of contemporary aerospace technology, it is essential that the "Systems Approach" generated in Tasks (02-06) be strictly adhered to, so that the other activities (10, etc., 20, etc., 30, etc.) must generate just the proper amount of information required for first order system synthesis and analysis.

II. SYSTEMS ANALYSIS

In order to fulfill its mission, i.e., Mars Fly-By, a deep space vehicle must communicate its data back to Earth. If the potential of laser communications can be fully exploited, this data transmission can be achieved in real-time. However, such high information bandwidths based on low power laser transmitters require extremely narrow beamwidths, i.e., 0.01-1.0 arc seconds. Therefore, a laser beam pointing system of great precision must be incorporated into the space vehicle-Earth mission communication and control complex.

If the complete system were required to operate "in vacuo" only, then the system problems would lie in the domains of high precision geometrical optics, servo dynamics with transit time and observer-target motion computation, and electro-optical tracking techniques. The presence of the Earth's atmosphere, however, completely modifies the systems aspects of laser communications and pointing control since "in vivo" propagation involves consideration of the influence of extraneous noise sources on the one hand, and the stochastic alteration of the geometrical and physical data of electromagnetic propagation on the other.

This section will describe the results of systems analysis and synthesis to date, corresponding to Tasks 02 and 03 (cf. Section IB), beginning with deep space radio communications and deep space laser communications "in vacuo". Thereafter, various system configurations and other aspects of systems analysis are described. A detailed description of atmospheric phenomena and their influence on light propagation is given in Section III.

A. DEEP SPACE RADIO COMMUNICATIONS

The NASA Deep Space Instrumentation Facility (DSIF) with headquarters at the Jet Propulsion Laboratory and principal station at Goldstone, California, is probably the best representative of contemporary deep space radio communication systems. Its evolution has been marked by an increasing sophistication of techniques with attendant advances in techniques for data acquisition, command, tracking, and data handling, as well as increased precision and performance for various subsystems such as antennas, transmitters, and receivers. Ground transmitter powers have increased from tens to hundreds of kilowatts, and spacecraft transmitter powers from 3-4 to 50 watts. Both ground and spaceborne antennas have been boosted by several decibels, and ground system noise temperatures have dropped more than 1000°K to well below 100°K, Ref. (2).

The performance of the NASA DSIF is shown in Table I, cf. Ref. (2), p. 55.

According to John W. Thatcher, Manager, Deep Space Network, J. P. L., using digital techniques, modulation efficiencies of about six cycle per bit (with unity S/N ratio per bit) have been achieved, and it is hoped that this will be reduced to about three cycles per bit in the future which is very close to Shannon's ideal information-theoretical limits, Ref. (2), p. 55. Hence, as the bottom line in Table I shows, present-day radio link systems are performance limited in their data rate capability both forthe present and the future.

For comparison, Table II presents some communication system requirements for various space missions in order to transmit good-quality, real-time television from the moon, facsimile pictures from Mars at the maximum Earth-Mars distance, and significant data from the edge of the solar system, Ref. (3), p. 35.

In order to match the mission performance requirements of Table II with the DSIF capabilities of Table I, the techniques of on-board data processing can be used, i.e., with information storage, a spacecraft can take a lot of data in a short time and retransmit back to earth at a slower rate, Ref. (2), p. 56, Ref. (3), p. 42. In the Mariner Mars fly-by mission, spacecraft TV pictures will be stored on magnetic tape and relayed back to earth at a much lower data rate. Where real-time video transmission is required, such as for the Ranger and Surveyor missions, frame rate and line-scan rate are tailored to the real-time transmission requirements, Ref. (11), p. 72.

It is clear that present-day deep space radio communications cannot provide the high information density real-time data transmission rates needed for all future unmanned and manned space missions, cf. Ref. (2), p. 63, Ref. (3), pp. 35-48, Ref. (10). Successful implementation of deep space laser optical communications systems will therefore fill a real need of the space exploration program.

B. DEEP SPACE LASER COMMUNICATIONS "IN VACUO"

Although many types of mission applications are contemplated for laser communication links (earth-vehicle, vehicle-earth, vehicle-vehicle, etc.), the space-to-earth link is truly representative of the widest class of problems, and should materialize the soonest to fulfill the U. S. NASA Aerospace program of the 1965-70 period, Ref. (1). Deep space radio communications has successfully met the space communications challenge of the past decade and will continue to be the principal telemetry and control link for space vehicles for the next

TABLE I

Typical Values for Presently Attainable Deep Space Communication Systems

	Spacecraft-to-Earth Link				Earth-to-Spacecraft Link			
	Moon	Venus	Mars	Edge of Solar System	Moon	Venus	Mars	Edge of Solar System
Distance from Earth (Mi)	2.5×10^5	3.7×10^7	1.4×10^8	4.4×10^9	2.5×10^5	3.7×10^7	1.4×10^8	4.4×10^9
Space loss (db.)	212	255	267	297	212	255	267	297
Modulation loss (db.)	4	4	4	4	8	8	8	8
Miscellaneous System loss (db.)	4	4	4	4	4	4	4	4
Spacecraft Antenna gain (db.)	26	26	23	34	0	0	19	31
Ground Antenna gain (db.)	53	53	53(61) ***	61	51	51	51	51
Transmitting power (watts)	10	3	10	50	10^4	10^5	10^4	10^5
Receiver noise spectral density (dbm/cps)	-174	-181	-181	-181	-164	-164	-164	-169
Performance margin (db.)	6	6	6	6	43	12	9	6
Data rate (bits/sec.)*	7.1×10^5	56	5.6**	2.2	1	1	1	1

* Bit error rate 5×10^{-3} for spacecraft-to-earth link, 1×10^{-5} for earth-to-spacecraft link

**Data rate will be 35 bits per sec. for later Mars probes when 61-db. antenna is available

***61-db. antenna will be available for later Mars probes.

TABLE II

Earth-Space Communication Links

Parameter	Typical Satellite	Lunar Orbiter w/TV	Lunar Lander w/TV	Mars Orbiter w/Facsimile	Probe to Edge of Solar System w/Cosmic-Ray Counter
Range (km.)	4×10^3	4×10^5	4×10^5	4×10^8	4×10^{10}
Ground Antenna Gain	10^3	10^5	10^6	10^6	10^6
Ground Antenna Diameter (ft)	40	85	250	250	250
Spacecraft Antenna Area (m^2)	0.05	7	2.5	25	25
Spacecraft Antenna Beamwidth (deg.)	Omnidirectional	2.2	3.6	1.2	1.2
System Temperature (deg.K)	400	220	400	25	25
Spacecraft Radiated Power (watts)	200	20	10	150	150
Frequency (gc.)	0.1-0.4(0.38)	2.3	2.3	2.3	2.3
Video Bandwidth for 30-db. S/N (cps)	4×10^6	10^6	10^6	2.5×10^3	
Bandwidth for 20-db. S/N (coded transmission, cps)	not used	10^7	10^7	2.5×10^4	2.5
One-Way mission time	20 min.	3 days	3 days	200 days	6 years *

* with electric propulsion

few years, Ref. (2). However, it was shown that upcoming space mission requirements cannot be met in real-time by radio links, and therefore, a real need exists for the development of deep space communications based on the new laser technology. Noteworthy discussions of the potential of laser communications have been given by Oliver, Ref. (12), Luck, Ref. (13), Megla, Ref. (14), and Brinkman, Pratt, and Vourgourakis, Ref. (15), among others.

"In Vacuo" communications refers to propagation in "free-space" without consideration of enhancement or interference due to propagation media, extraneous background radiation sources scattering phenomena, etc. The influence of these other factors will be considered in later memoranda, and it will be seen that their effects and consequences completely modify the systems aspects of laser communications. From a system point of view, however, the "in vacuo" or "free-space" analysis is valuable in that it defines ideal communications system performance under no interference.

The performance of a free-space laser communications link can be described in terms of the following system equations with specific values assumed for certain system parameters to provide concrete illustrative values; for details, see Refs. (12), (13), (14).

TABLE III

Laser Communication System Performance Equations

Parameter	Equation	Remarks
Beamwidth, θ	$\theta = \frac{\lambda}{d}$ (radians)	λ = wavelength d = telescope diameter
Solid Angle, Ω	$\Omega = \theta^2$ (steradians)	
Antenna Gain, G	$G = \frac{4\pi d^2}{\lambda^2} = \frac{4\pi}{\Omega}$	Neglect losses
Received Signal, S_R	$S_R = \frac{P_T G_T G_R \lambda^2}{(4\pi r)^2}$ (watts)	P_T = transmitter power r = range

TABLE III (cont'd.)

Parameter	Equation	Remarks
Transmitter Power, P_T	P_T = 1.0 watt	Illustrative Example
Wavelength, λ	λ = 6328 Å	Illustrative Example
Information Bandwidth, B	B=7.2 mcs.=7.2x10^6 cps	Illustrative Example
Channel Capacity, C	$C=B \log_2(1+\frac{S}{N})$ $(\frac{bits}{sec.})$	$\frac{S}{N}$=Signal-to-Noise ratio
Minimum Detectable Signal, S_R min.	$S_{R_{min}} \frac{mC}{\eta} hf$ (watts)	m=electrons per bit η =quantum efficiency hf=energy per quantum
Quantum Efficiency, η	η = 20% = 0.2	Illustrative Example (14)
Electrons per Bit, m	m = 20	Illustrative Example (14)
Quantum Energy, hf	hf=3.16x10^{-19} watt-sec.	Illustrative Example
Signal-to-Noise Ratio, $\frac{S}{N}$	$\frac{S}{N} \equiv 20$	Illustrative Example
Capacity, C	C=3.2x10^7 $\frac{bits}{sec.}$ for $\frac{S}{N} \simeq 20$	Illustrative Example

TABLE III (cont'd.)

Parameter	Equation	Remarks
Maximum Range, $r_{max.}$	$r_{max.} = \frac{9.5}{\theta^2} \frac{P_T 7}{hfC}$ (km.)	λ-microns, θ-arc secs. P_T-watts, hf-watt sec. $C - \frac{bits}{sec.}$ m=20 e^-/bit, Ref.(6)
Transit Time, Δt	$\Delta t = \frac{r}{c}$ (sec.)	Light velocity $c=3\times10^8 \frac{meters}{sec.}$
Two-Way Capacity, C'	$C' = \beta C = \beta B \log_2 (1+\frac{S}{N}) \frac{bits}{sec.}$	Two-Way Communication $0 \leq \beta \leq 1$, Ref. (14)
Degradation, β	$\beta = \frac{T}{T+\Delta t} = \left(1+\frac{r}{cT}\right)^{-1}$	T ≡ Message Time, Ref. (14)

The following chart, Table IV, based on the previous equations and illustrative parameter values, tabulates some laser communications system performance parameters for three assumed values of antenna (telescope) beamwidth, namely: 1.0, 0.1, 0.01 arc seconds. Assuming diffraction-limited optics, for relatively modest apertures by microwave standards, Table II, the theoretical values of antenna gain are more than 110 db, 130 db, and 150 db respectively. Similarly, these ultra-narrow beamwidths subtend quite small linear distances on the Earth even from Mars at fly-by at minimum distance (0.524 A.U.) (e.g., Mariner, Mars C, Voyager), namely: 3,800 km. (2,355 miles), 380 km. (235 miles), 38 km. (23.5 miles). The maximum range is tabulated in km. and A.U. (Astronomical Unit), assuming a receiving aperture on Earth of the Palomar type, 200 inch or 5.1 meter diameter. Comparison of this data with the mission requirements tabulated in Table II shows that the one arc sec. beamwidth satisfies

lunar mission requirements, and the 0.01 arc sec. beamwidth system enables full coverage of the Mars mission and beyond, i.e., Uranus. A 20 db reduction in C would increase r max by plus 10 db, yielding range coverage to the edge of the solar system (between Uranus and Pluto). Of course, these figures are theoretical only, applying to free-space "in vacuo" propagation with perfect beam pointing. "In Vivo" propagation will be discussed in a subsequent memorandum.

TABLE IV

Examples of Earth-Space Communications Links

Parameters	Beamwidths, θ (arc sec.)		
θ (arc sec.)	1.0	0.1	0.01
d (meters)	0.131	1.31	13.1
Ω (sterad.)	2.35×10^{-11}	2.35×10^{-13}	2.35×10^{-15}
G (numeric)	5.34×10^{11}	5.34×10^{13}	5.34×10^{15}
$l = r\theta$ (meters) r = 0.524 A.U. Mars, min.	3.8×10^{5}	3.8×10^{4}	3.8×10^{3}
S_R (watts) Mars to Palomar d_R = 200" = 5.1 m.	0.99×10^{-10}	0.99×10^{-8}	0.99×10^{-6}
r_{max} (km.)	8.45×10^{5}	8.45×10^{7}	8.45×10^{9}
r_{max} (A.U)	0.565×10^{-2}	0.565	56.5

Megla, Ref. (14), has computed the effect of transit time on the performance of the laser communication link, which is shown in Table V below. This effect also enters into the performance of a two-way cooperative beam pointing system. The chart shows the minimum permissible durations of messages for degradation values of $\beta = 0.5$ (3 db) and $\beta = 0.8$ as a function of range to various planets for a two-way link. It is clear that transit time is a significant factor in both the communications and control (pointing) aspects since it occurs both in the closed loop (cooperative) performance and the open loop (aberration due both to observer and target motion) performance. However, since the pointing control system bandwidths are much smaller than communications information bandwidths, the message duration factor is less critical for beam pointing performance.

TABLE V

Transit Time Effects on Communications

Planet	r_{max} (A.U.)	r_{min} (A.U.)	Δt max.	Δt min.	T message $\beta = 0.5$	T message $\beta = 0.8$
Mercury	1.387	0.613	11.53 min	5.08 min	11 min.42sec	52min30sec
Venus	1.723	0.277	14.3 min.	2.3 min.	14 min 30 sec	1 hr 2.5min
Mars	2.524	0.524	21.1 min.	4.35 min	20 min 48sec	1hr 31.7min
Jupiter	6.203	4.203	51.6 min	35.0 min	45 min	3 hr 33 min
Saturn	10.539	8.539	1.46 hr	1.18 hr	1 hr 24 min	6 hr 15 min
Uranus	20.191	18.191	2.8 hr	2.52 hr	2 hr 47 min	11hr 56 min

As noted in Ref. (14), p. 315, the transit limitations are independent of carrier frequency, and therefore, the data of Table V are applicable to both radio and laser communication links.

The problems associated with laser communications "in vivo" will be described in the next report.

C. BEAM POINTING SYSTEM VARIABLES

As previously noted, laser communications "in vivo" requires drastic modifications in system philosophy and system configurations since the presence of an atmosphere and extraneous radiation sources completely alter free-space system performance. Beam pointing system philosophy is similarly affected, and therefore, this section will consider the variables involved in laser communications and laser beam pointing "in vivo".

In common with other tracking systems such as stellar guidance and radar, the laser beam pointing system must fulfill the functions of acquisition (search, detect, and acquire) and tracking (including stabilization, closed loop operation, smoothing, and prediction).

The factors involved in the pointing system are shown schematically in Figure 3. It is seen that they include the spacecraft coordinate and attitude reference system, the earth coordinate and attitude reference system, the common celestial-inertial reference frame (stars, sun, planets, moons, etc.), the interplanetary media including planetary atmospheres, and the characteristics of the laser communications and beam pointing systems. These factors are both static (including stochastic and anomalous conditions) and dynamic (including the kinematic factors of transit time, Doppler shift, aberration, etc.).

Viewed from the spacecraft, these factors are included in the three major problem areas defined as program objectives, Section IA.

However, it is clear from Figure 3 that these spacecraft-oriented problem area descriptions are embedded within the framework of the total communications and beam pointing system, and therefore, a total system approach is required to generate an "In Vivo" solution including the Earth's atmosphere and all of the other system uncertainties. A simple first order analysis of the errors and uncertainties listed in Figure 3 demonstrates that a laser beam pointing system based on direct analogy with conventional open-loop astronomical or star-tracking techniques could not possibly fulfill the mission requirements for spacecraft laser beamwidths from 1.0-0.01 arc seconds. The uncertainties due to the turbulence phenomena of the Earth's atmosphere alone, i.e., the well-known "astronomical seeing" problem, render a simple open-loop pointing system unacceptable for the ultra-narrow beamwidths, cf., Section III, "Laser Propagation Through the Atmosphere".

FIXED STARS

STELLAR COORDINATE SYSTEM
Errors & Uncertainties

Stellar Catalog Positions:	0.03"-0.13"
Astronomical Precession:	10^{-11} °/hr.
Parallax Corrections:	0.77"(α -Centauri)
Other Uncertainties:	Physical Classifications Apparent Motions Inertial Coordinates Earth Coordinates

TARGET PLANET

PLANET COORDINATES
Errors & Uncertainties:
Inertial Coordinates: See Below
Angular Diameters at 1 A.U.:

Mercury:	±0.02"
Venus:	±0.03"
Mars:	±0.015" (Equat.) ±0.01" (Polar)
Jupiter:	±1.4" (Equat.,Polar)
Saturn:	±1.4" (Equat.) ±1.72" (Polar)

Other Uncertainties: Mass & Light Centers
Illumination Phases
Magnitudes, Albedos,
Atmospheric Prop.
Orbital Parameters
& Velocities
Angular Rates

INTERPLANETARY ENVIRONMENT
Uncertainties: Interplanetary Atmosphere, Radiation Belts and Zones, Meteor and Asteroid Distributions, Effects of Solar Events such as Sunspots and Flares.

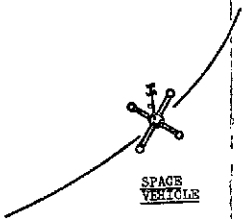

SPACE VEHICLE

ELECTRODYNAMICS AND PROPAGATION
Uncertainties: Transit Time, Aberration due to Observer Motion and Target Motion, Angle of Arrival, Polarization, Intensity, Phase Distributions.

DSIF COORDINATES
Errors
Doppler Velocity: 0.03 meter/sec.
Range: < 50 miles
Time Signal Settings: 3×10^{-3} sec.
Timing Drift Errors: 1 sec./several years

CELESTIAL & INERTIAL DATA
Star Trackers: 0.1-1 sec.
Horizon Trackers: < 1 minute
Platform Drift: 0.001°/hr.

POINTING SYSTEM
Uncertainties:
Reference Axes
Beam Mess. & Positioning
Boresight
Structures, Data Readout,
Control System, Computer

EARTH COORDINATES
Errors & Uncertainties:
Inertial Coordinates: See "Solar System"
Geodetic Coordinates:
Equatorial Radius: ±11 meters
Land Mass Distances: ±0.01 naut. mile
Other Uncertainties: Reference Ellipsoid, Geoid, Optical Diameters, Spin Rates, Local Vertical Deflections, Gravity Anomalies

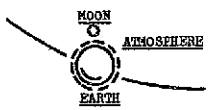

POINTING SYSTEM
Uncertainties:
See "Space Vehicle Pointing System" except to a lesser extent

ATMOSPHERE
Uncertainties:
Clouds and Precipitation, Transmission, Elevation
Absorption: Function of H_2O, CO_2, O_3
Mass Refraction: 0-35' min. 21 sec. (Zenith Angles: 0-90°)
Scattering: Rayleigh and Mie (below 20 km.)
Turbulence: Scintillation, Shimmer and Coherence Degradation due to Differential Refraction

Interference Sources: Solar Radiation Scattering, Lunar Elevation and Phase, Stars and Planets, Auroral Activity, Airglow Emissions, Thermal Emission, Cloud Reflections, Noctilucent Clouds, Scattered Moonlight, Night Glow, Earth Albedo

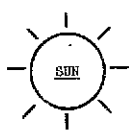

SOLAR SYSTEM

INERTIAL COORDINATE SYSTEM
Errors & Uncertainties
Astronomical Unit: ±150 km.
Universal Time: < 1 sec./yr.
Velocity of Light: ±0.3 km./sec.
Aberration Constant: ±0.0015 sec./A.U.
Planetary Positions:
Mercury, Venus, Earth-Moon, Mars: 100-150 km.
Certain Asteroids: 150 km.
Jupiter, Saturn: 600 km.
Uranus, Neptune, Pluto: 1000-3000 km.

Other Uncertainties: See "Planet Coordinates" Above

* See Table I for Details

Figure 3. Factors Affecting Laser Beam Pointing System Accuracy *

30 A

B

It is clear that the ultimate solution to laser beam pointing problems will be based on a hybrid combination of open-loop (non-cooperative) and closed-loop (cooperative) techniques, Ref. (7), pp. 11-12. These solutions will be analyzed in greater detail in subsequent reports.

D. PARTIAL SUMMARY OF POINTING SYSTEM ERRORS AND UNCERTAINTIES

For future reference, a partial summary of errors associated with the pointing system factors and variables is given below. This list will be revised, enlarged, and up-dated as more data become available. References cited in the list are identified (wherever possible) in the alphabetical list immediately following the summary.

TABLE VI

Errors and Uncertainties (Ref. Figure 3)

Systems, Factors, Variables, Parameters, and Constants	Error Magnitude		Data Reference
Inertial Coordinate System			
Astronomical Unit (A.U.)	± 450 km.		Naqvi & Levy, p.159
Universal Time (UT)	<1 sec./yr.		" " " ,p.159
Velocity of Light (c)	± 0.3 km./sec.		" " " ,p.160
Planetary Aberration Constant (θ)	± 0.0015 sec./A.U.		" " " ,p.160
Planetary Positions:	km.	Angle at 1 A.U.	" " " ,p.160
Mercury	100	0.1 sec.	
Venus	150	0.2	
Earth-Moon System	100	0.1	
Mars (Newcomb & Ross)	150	0.2	
Mars (Duncombe & Clemence)	100	0.1	
Certain Asteroids	150	0.2	
Jupiter	600	0.8	

TABLE VI (cont'd.)

Systems, Factors, Variables, Parameters, and Constants		Error Magnitude	Data Reference
Inertial Coordinate System (cont'd.)			
Saturn	600	0.8	
Uranus	1000	1.0	
Neptune	1500	2.0	
Pluto	3000	4.0	
Other Uncertainties:	Planetary Diameters*, Mass Centers, Light Centers, Illumination Phases, Magnitudes, Orbital Velocities, Diurnal Angular Rate, Annual Period. * See Planet "Coordinates"		
Stellar Cordinate System			
Stellar Catalog Star Positions	0.03 - 0.13 sec.		Naqvi & Levy, p.156
Astronomic Precession	10^{-11} deg./hr.		Space/Aeron., 1961 p.146
Parallax Corrections	0.77 sec. (Alpha Centauri)		Larmore, pp. 41-42
Other Uncertainties:	Physical Classifications, Magnitudes, Apparent Motions, Inclination of Invariable Plane		

TABLE VI (Cont'd.)

Systems, Factors, Variables, Parameters, and Constants	Error Magnitude	Data Reference
Planet Coordinates		
Angular Diameters at 1 A.U.	Arc Sec.	Naqvi & Levy, p.161
Mercury	±0.02	
Venus	±0.03	
Mars-Equatorial	±0.015	
Mars-Polar	±0.01	
Jupiter-Equatorial	±1.4	
Jupiter-Polar	±1.4	
Saturn-Equatorial	±1.14	
Saturn-Polar	±1.72	
Other Uncertainties:	Inertial Coordinates, Mass and Light Centers, Illumination Phases, Magnitudes, Albedos, Atmospheric Properties, Orbital Parameters and Velocities, Angular Rates.	
Earth Inertial Coordinates		
Planetary Position (km.)	100 km.	Naqvi & Levy, p.160
Planetary Position (Angle at 1 A.U.)	0.1 sec.	" " " , p.160
Optical Angular Diameters:	Arc Sec.	" " " , p.161
Infrared-Clear-Equatorial	±0.001	
" " Polar	±0.001	
Infrared-Cloudy-Equatorial	±0.002	
" " Polar	±0.002	

TABLE VI (Cont'd.)

Systems, Factors, Variables, Parameters, and Constants	Error Magnitude	Data Reference
Earth Inertial Coordinates (Cont'd.)		
Visible (0.55μ)-Equatorial	±0.003	
" " Polar	±0.003	
Earth Spin Rate Fluctuations	1.7×10^{-6} deg./hr.	Space/Aeron.,1961,p.146
* Difference in Inertial and Sidereal Spin	10^{-6} deg./hr.	" " "
* Proper Motion of Stars	3.3×10^{-9} deg./hr.	" " "
Astronomic Precession	10^{-11} deg./hr.	" " "
* Inertial Angular Velocity of Earth-Centered Inertial Frame due to Astronomic Precession	2.5×10^{-6} deg./hr.	" " "
* Inertial Angular Velocity of Earth-Centered Inertial Frame Viewed from Earth-Satellite	2.4×10^{-7} deg/hr.	" " "
* Inertial Angular Velocity of Helio-Centric Inertial Frame Viewed from Earth	4.8×10^{-10} deg./hr.	" " "

Other Uncertainties: Earth Orbital Parameters (Inertial Coord. System)

* These represent effects to be considered rather than errors.

TABLE VI (Cont'd.)

Systems, Factors, Variables, Parameters, and Constants	Error Magnitude	Data Reference
Earth Station Geodetic Coordinates		
Motion of Equator and Poles in Crust	1 sec.	Newton, p. 4
Error in Earth's Equatorial Radius	±11 meters	Tross, p.940
Geodetic Land Mass Information	±0.01 n.m.	Space/Aeron., 1961, p. 146
Other Uncertainties:	Misalignment between axis of reference ellipsoid and geographic polar axis, geoid and ellipsoid contours, deflections of local vertical and gravity anomalies.	
* effects to be considered rather than errors.		
Space Vehicle DSIF Coordinates		
Microwave Doppler Velocity	0.03 meter/sec.	Thatcher, p. 58
Range	$<$ 50 n.m.	" p. 58
Time Signals Settings	3×10^{-3} sec.	" p. 57
Timing Drift	2 pts. in 10^{10}/yr.	" p. 57

References to Table VI

L. Larmore, "Celestial Observations for Space Navigation", pp. 37-42, Aero/Space Engineering, Jan. 1959.

A. M. Naqvi, R. J. Levy, "Some Astronomical and Geophysical Considerations for Space Navigation", pp. 154-170, I.E.E.E. Transactions on Aerospace and Navigational Electronics, Vol. ANE-10, No. 3, Sept. 1963.

R. R. Newton, "Astronomy for the Non-Astromer", IRE Transactions on Space Electronics and Telemetry, pp. 1-16, March 1960.

Space/Aeron. 1961, "Space Guidance Highlighted at ARS Meeting," pp. 143-150, Space/Aeronautics, Vol. 36, No. 4, Nov. 1961.

J. W. Thatcher, "Deep Space Communication", pp. 54-63, Space/Aeronautics, Vol. 42, No. 1, July 1964.

C. Tross, "Astronomical Constants and Their Importance in Lunar Trajectory Determinations", ARS Journal, pp. 938-941, October 1960.

E. GENERAL BEAM POINTING SYSTEM CONSIDERATIONS

The overall accuracy of the Laser Beam Pointing System is determined by all of the factors shown in Figure 3. A useful first approximation is obtained by considering the "In Vacuo" situation in which case the analysis from both ends of the communications link is symmetrical. Then, it is sufficient to consider the system involved in the space vehicle, i.e., the three major problem areas cited in Section IA, namely:

(1) Techniques for detecting and establishing suitable reference axes from which to derive pointing information for the laser beam.

(2) Techniques for measuring and positioning the optical pointing axis with respect to the reference axes and/or with respect to incident radiation from the desired cooperative second terminal.

(3) Techniques for maintaining boresight between the optical and mechanical axes of the laser.

With regard to the first problem of establishing suitable reference axes, the Kollsman Goddard Experimental Package of the OAO utilizes a course-fine guidance system in conjunction with the 38-inch telescope, providing the spacecraft's stabilization and control system with a sighting error of about one second of arc, Ref. (16). The optical guidance subsystems being provided by Kollsman for the Apollo mission includes a sextant, a scanning telescope, and a map-and-data viewer to permit the observation of stars, planets, the moon and landmarks on the earth and moon to determine directions in space, Ref. (17). Similarly, six Kollsman star trackers are used on each OAO space vehicle as part of the attitude stabilization and control system, Ref. (18).

Since systems of these types are one-way systems, they are essentially open-loop in terms of the inputs, requiring therefore very high precision in their optics and readouts. (Of course, the inner tracking systems make use of closed loop techniques, but the exterior signal and noise input sources are non-cooperative, i.e., one-way). For the beam pointing system, the use of cooperative techniques offers the potential of a considerable reduction in the accuracy required of the reference axes' systems. In other words, in the two-way system, the reference axes provide the framework for coarse pointing during acquisition with fine pointing controlled by the cooperative laser beacons.

The problem of measuring and positioning the optical pointing axis with respect to the reference axes and/or cooperative radiation, is coupled to the laser transmitter optical system configuration. The chart of Table IV shows that for one arc second, the aperture is relatively small (5.16 inches), but for 0.1 arc second, it is 51.6 inches (about one and a half times the size of the GEP mirror), and for 0.01 arc second, it is 516 inches. The latter two will undoubtedly be implemented by motion of the laser beam at the focus, rather than paraboloid slewing, or else by means of phased coherent optical arrays, Ref. (19). Hence, although angle transfer techniques of the order of 0.01 arc second are feasible, the dependence on the laser transmitter optics requires further investigation. However, the problem is somewhat mitigated by the fact that coherent laser radiation allows for greater precision in measurement due to superior independence of wavelength, in interferometry for example. The problems normally associated with reaction torques and counterbalancing can be considerably avoided by the use of fine optical beam deflection techniques such as are described in Section IV below.

In the space vehicle, reference axes will be derived from the celestial-inertial sensors. The laser beam pointing mechanism (paraboloid motion or focal motion or phased array control) can be measured and positioned relative to the reference axes utilizing the high precision optical and angular transfer links already under development for the OAO GEP in the case of 1 and 0.1 arc second beams. For the 0.01 arc second beamwidth, more precise techniques based on interferometer fringe displacement can be exploited (accurate to about 0.02 arc second). The maintenance of boresight between the optical and mechanical axes can be achieved by optically sampling the laser beam and comparing it with an optical surface on the mount, either in an autocollimation mode or an interferometric configuration for the highest precision. Of course, the boresight alignment maintenance must be automatic and therefore implemented by a servo control. Since adequate signal-to-noise ratios can be expected, good closed-loop operation should be possible.

In connection with beam positioning and boresight maintenance, the linearity, sensitivity, and stability of the former and sensitivity and response time of the latter and critical since the kinematic lead compensation for aberration and transit time is an essentially open-loop process. The allowable errors will be some fraction of the beamwidth and the linearity will be a function of the magnitude of the lead corrections.

As noted at the beginning of this section, the "In Vacuo" situation may be described in terms of the three major problems viewed in the space vehicle as cited above. In the "In Vivo" situation including the Earth's atmosphere and interplanetary media, the two ends of the link (space vehicle and Earth) lose their bilateral symmetry because of atmospheric phenomena, cf. Section III of this report.

A preliminary analysis of the total situation leads to the diagrammatic description of Laser Beam Pointing shown in Figure 4. The statement of the problem in the upper half of the diagram reflects the previous discussion and the factor sets previously shown in Figure 3. The "Conclusions and Solutions" are generalized from various analyses of both laser communications and laser pointing, Refs. (3), (6), (7), (15), as well as the highly developed microwave radio and radar technology, Refs. (2), (3).

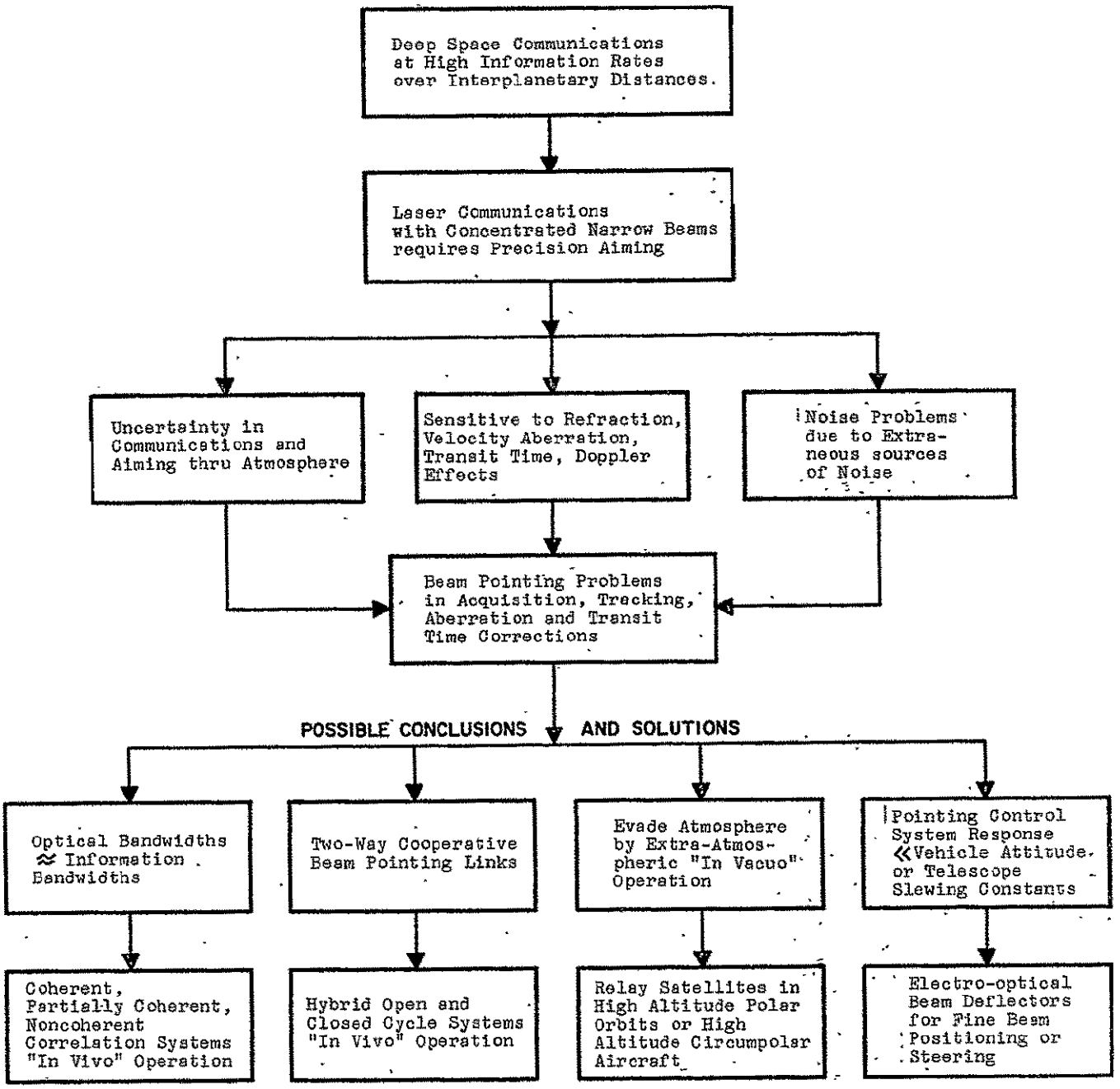

Figure 4. "In-Vivo" Laser Beam Pointing Problems and Solutions

The various considerations associated with the blocks shown in Figure 4 will receive detailed treatment later in this report and in other reports. Aside from the question of "In Vacuo" versus "In Vivo" operation, a major consideration of the laser beam pointing problem is the question of "one-way non-cooperative pointing" versus "two-way cooperative operation".

The preliminary systems analysis of laser beam pointing factors shown schematically in Figure 3 categorizes them into nine major sets, namely: (1) spacecraft laser beam pointing, (2) earth station cooperative laser beam pointing, (3) spacecraft position, velocity, attitude, and attitude rate, (4) earth station geodetic coordinates, (5) earth's position, velocity, and angular rates, (6) inertial-stellar coordinate frames, (7) atmospheric refraction and turbulence, (8) interplanetary environment, and (9) target planet's position, velocity and angular rates.

A systems approach requires consideration of the manifold sources of uncertainty associated with these nine categories as previously described. Aboard the spacecraft, the three major problems associated with reference axes, laser beam pointing and measurement, and opto-mechanical boresight maintenance cut across most of these categories either during the acquisition or tracking phases, or both.

According to the precepts of general systems theory, systems of the class belonging to the laser beam pointing problem may be classified into one of three types: (1) open-cycle (non-cooperative), (2) closed-cycle (cooperative), (3) hybrid (combination open and closed-cycle), Refs. (8), (20). In each of these categories, it is further possible to subdivide into many different systems as a function of the transmitter and receiver, the optics, the detection schemes, the scanning mechanisms, the tracking servos, and the data processors of the archetype laser beam pointing system.

In fact, the situation is quite analogous to the use of error detection and error correction codes in communication systems, namely, the use of algebraic and sequential coding (open loop), feedback correction (closed loop), and hybrid (combined coding and feedback), Ref. (21). This analogy has been employed in the analysis of star tracking systems, Ref. (22). A family tree of celestial sensors of the types used for establishing reference axes in airborne and space vehicles (such as the Kollsman systems previously described) will be presented in later studies on, "Reference Axes".

A family tree chart of these classes of laser beam pointing systems is shown in Figure 5. The chart below illustrates the evaluation factors which an intensive study program should yield. The equipment complements for each class are illustrative of the system configurations, but not exhaustive in terms of all possible types, modes, etc. The source of error are attributable to the sources of uncertainty shown in terms of the nine categories in Figure 3. Celestial sensors are of the types discussed in Ref. (23). Mission requirements are correlated with the laser communication system requirements, examples of which were given in Section II A, B.

The most flexible system appears to be the hybrid (combination open-and-closed loop) based on the joint use of reference axes' coarse pointing information and acquisition, followed up by a cooperative system fine acquisition and tracking mode. In such a system, maximum use of coding, correlation, and prediction procedures can be employed to optimize data transmission capacities, procedures, propagation conditions, etc.

The celestial and inertial sensors establish reference axes for the space transmitter, and their counterpart on earth (the astronomical geodetic observatory) establishes the reference axes for the receiver portion on the ground. These reference axes are essential in all of the three classes of system noted above (open loop, closed loop, and hybrid), since they define the geometry and the kinematics of the inertial coordinate, space vehicle, and earth reference frames relative to the celestial reference frame of the fixed stars. However, the accuracy of these data depends on the system configuration. For an open-cycle (non-cooperative) system, the accuracy of angle data is of the order of one-tenth of the fine tracking beamwidth. For the pure closed-cycle (cooperative and hybrid systems, an accuracy of the order of one-tenth of the coarse acquisition beamwidth seems to be satisfactory. These accuracy requirements will be established in detail in the course of the system analyses (Tasks 03-06).

The choice of celestial sensors (including associated inertial platforms) is a function of the mission (i.e., near-earth, near-moon, satellite, near-planet, deep space, etc.). The mission likewise determines the parameters of the laser communication link, with wider beamwidths (one second and up) employed for the smaller ranges and the narrow beamwidths (0.1-0.01 seconds) being used for interplanetary exploration, etc. The optimal configuration is one which is best integrated with the laser communication system. (Further discussion of instrumentation for space navigation is presented in the article by S. Moskowitz and P. Weinschel of Kollsman's Space Division, (Ref. (23).

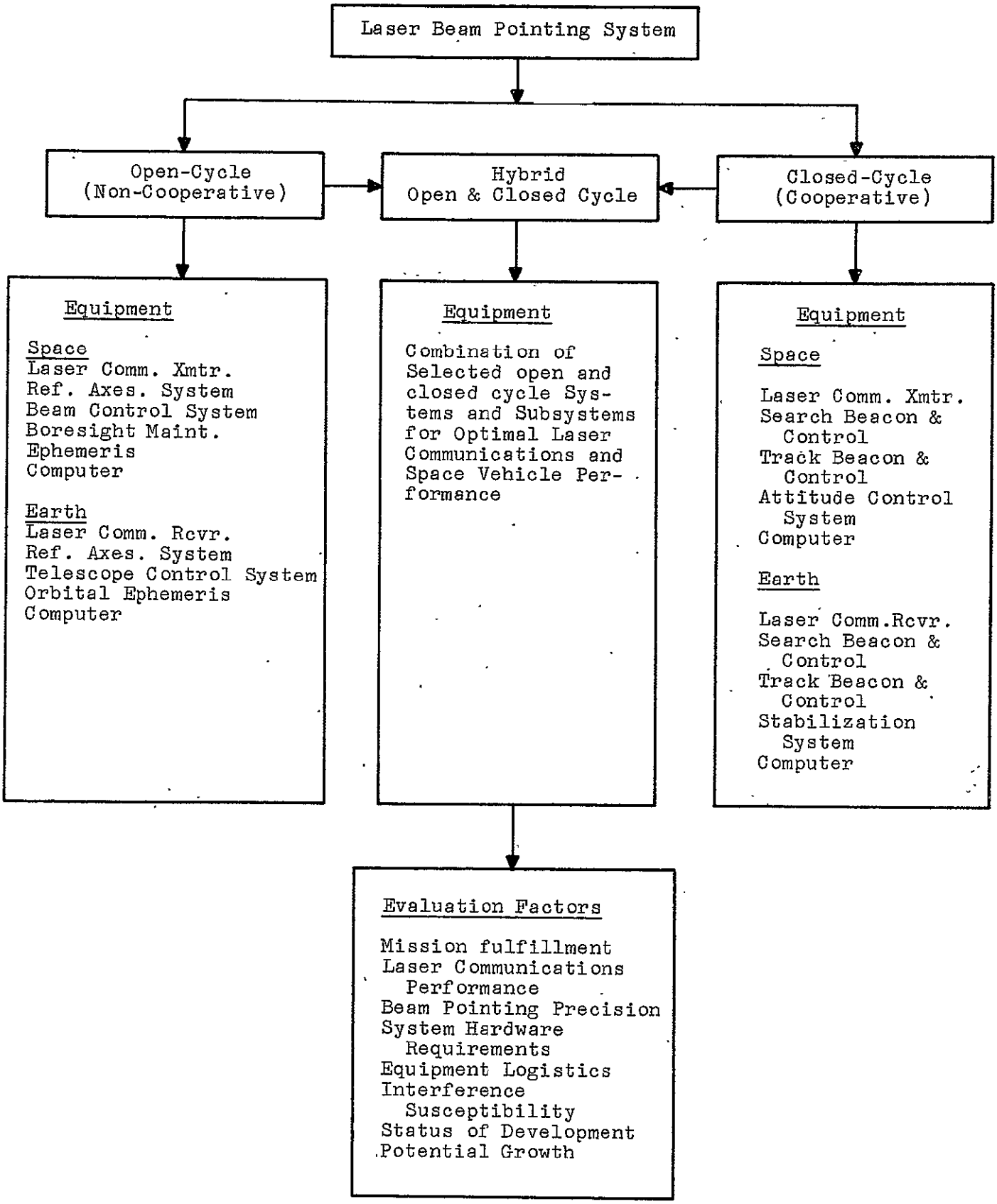

Figure 5. Laser Beam Pointing System Configurations

The operation of the open-cycle (non-cooperative) system is similar to the conventional astronomical procedure except that it takes place simultaneously in the space vehicle and on earth, using catalogs of stellar position and computer-controlled prediction techniques, Ref. (24). This technique appears to be feasible for near-earth missions using wider beamwidths, but error analysis and consideration of system complexity is required to establish the full range of missions for which such an approach is suitable. However, for deep space missions with beamwidths of one arc second or less, the present degree and number of system and factor uncertainties shown in Figure 3 appear definitely to preclude any possibilities of open-cycle operation "In Vivo".

A pure closed-cycle cooperative system uncomplicated by transit time problem is certainly feasible in principle, Ref. (25)-(27). However, the complications of narrow beamwidth, narrow frequency spectrum, and transit time render such systems impracticable for most important deep space missions because of the complexity of the search procedures and the lengthy duration of the search periods. The disadvantages are multiplied in the presence of atmospheric obscuration which can suddenly break "target lock", necessitating re-acquisition. Even using "coast" memory procedures, the re-acquisition process is still complicated by the factors noted above.

The structure of the Hybrid System configurations is derived from the techniques currently employed in microwave radar (e.g., NASA DSIF), IR detection theory, Ref. (28), star tracking systems, (Ref. (29), and airborne radar, Ref. (30). The composite character is required by the combination of high precision factors (narrow beamwidths, wide frequency spectra, space kinematics) and astronomical factors such as transit time, Doppler shift, atmospheric refraction, etc. These techniques are well-known to systems engineers from previous experience with celestial guidance, laser alignment and radar systems, and other microwave radar programs, and will be discussed below.

F. LUMPED AND DISTRIBUTED SYSTEMS

The preceding general considerations apply both to the "In Vacuo" and "In Vivo" cases. As previously noted, the "In Vacuo" condition is a special case of the "In Vivo" condition such that both ends of the link (space vehicle and Earth) are bilaterally symmetrical from a systems point of view. In other words, all of the system transfer functions (e.g., kinematic, electromagnetic, optical, inertial, etc.) are covariant with respect to a permutation transformation of space vehicle and Earth.

In the "In Vivo" case, this bilateral symmetry or covariance no longer applies because of the Earth's atmosphere and the interplanetary media. The exact nature of the reciprocity is described in Sections III A-F. Less technical discussions may be found in the literature, Refs. (6), (15), and (31). In addition, as previously discussed in Section II B, the interference due to extraneous noise sources is a severely limiting factor in the performance of laser communications "In Vivo", which is ignored in the "In Vacuo" analysis. These noise sources are also discussed below in Section III B.

As is the usual case in the real world, the "In Vivo" conditions demand conflicting solutions with the customarily ensuing need for compromise and trade-off analysis. Consideration of the interference due to extraneous noise sources leads to the conclusion that very narrow band receivers are required, i.e., optical bandwidths should be approximately equal to information bandwidths, cf. Figure 4, Refs. (6), (15), This constraint leads to the stipulation of the use of optical heterodyne receivers, analogous to microwave communications, i.e., coherent optical reception with narrow I. F. bandwidths (video versus 0.1 Å for incoherent systems). It is shown in Sections III A-F below that the effect of atmospheric differential refraction and turbulence causes a number of deleterious effects in laser beam propagation, namely, beam divergence, fluctuations in the angle of arrival (image dancing), fluctuations in received intensity (scintillation), and other conditions associated with the overall phenomenon commonly described in astronomy as "seeing conditions". Of particular importance is the degradation of phase coherence across the beam and the break-up of the beam into a small number of locally coherent patches with overall loss of spatial coherence, Refs. (6), (15), (31).

Now, reduction in "image dancing" and "scintillation" is best achieved by the use of larger receiving apertures or telescopes (as well as the choice of suitable sites), Section III A-F, Ref. (15). Conversely, the loss in received signal power when coherent optical heterodyne reception is used due to atmospheric degradation of phase coherence is decreased if smaller apertures are used, Section III A-F, Ref. (15). Brinkman et al, Ref. (15), conclude that for existing detector technology and earth-based operation with presently known atmospheric limitations, incoherent quantum counter laser communication systems are to be preferred over coherent systems. To quote, p.40: "Atmospheric transmission favors incoherent operation since larger apertures may be profitably used; heterodyne operation, if possible, would permit narrow-band (IF) filtering, which would be valuable for daytime and Mars background limited operation".

The situation is less serious for the Laser Beam Pointing System from one point of view since the control system bandwidths will be much smaller, i.e., much less than 100 c.p.s. Hence, higher signal-to-noise ratios in the presence of extraneous noise sources are easier to obtain, especially with the use of modulation techniques to cancel out steady state noise or slow fluctuation noise. Consequently, larger apertures can be used for the telescopes to reduce the effect of beam divergence, image dancing, and beam break-up in order to realize the pointing accuracy, cf. Section III A-F below. Nevertheless, further investigation of the effects of atmospheric phenomena on the beam pointing system accuracy is required in order to quantitatively evaluate performance. Since the atmosphere is not bilaterally symmetric, these investigations must be separately carried out for each end of the communication link, i.e., from space-to-earth and earth-to-space, as described later in this report.

Alternatively, one may consider more complex systems which can be optimized for the "In Vivo" conditions of atmospheric degradation and extraneous noise sources. Specifically, the microwave radar and communications fields have developed techniques for coping with scattering phenomena, i.e., bistatic radar as well as monostatic radar, tropospheric and meteoric scatter communications, and radio astronomical interferometry, Refs. (32)-(34). In addition, advances in adaptive filtering techniques, pattern recognition systems, adaptive antenna arrays, etc. suggest system configurations which may be used to counter the atmospheric degradation and scattering as well as provide spatial filtering against the extraneous noise sources analogous to optical filtering, Refs. (35), (36).

Accordingly, two classes of systems may be postulated, namely, "lumped" and "distributed". The "lumped" system corresponds to monostatic radar and the "distributed" system is essentially the counterpart of bistatic radar. From the point of view of general systems theory, Refs. (8), (20), these systems are related by principles of duality well-known in mathematics, physics, circuit theory and information theory, Refs. (37)-(40). In particular, the foregoing applies to the Earth station receiving system with some possible applicability to the space vehicle system.

The results of these considerations are summarized in Figure 6. The "Lumped System" class subdivides into the two types of detection philosophies, coherent and noncoherent, as previously discussed. For each of these subclasses, there

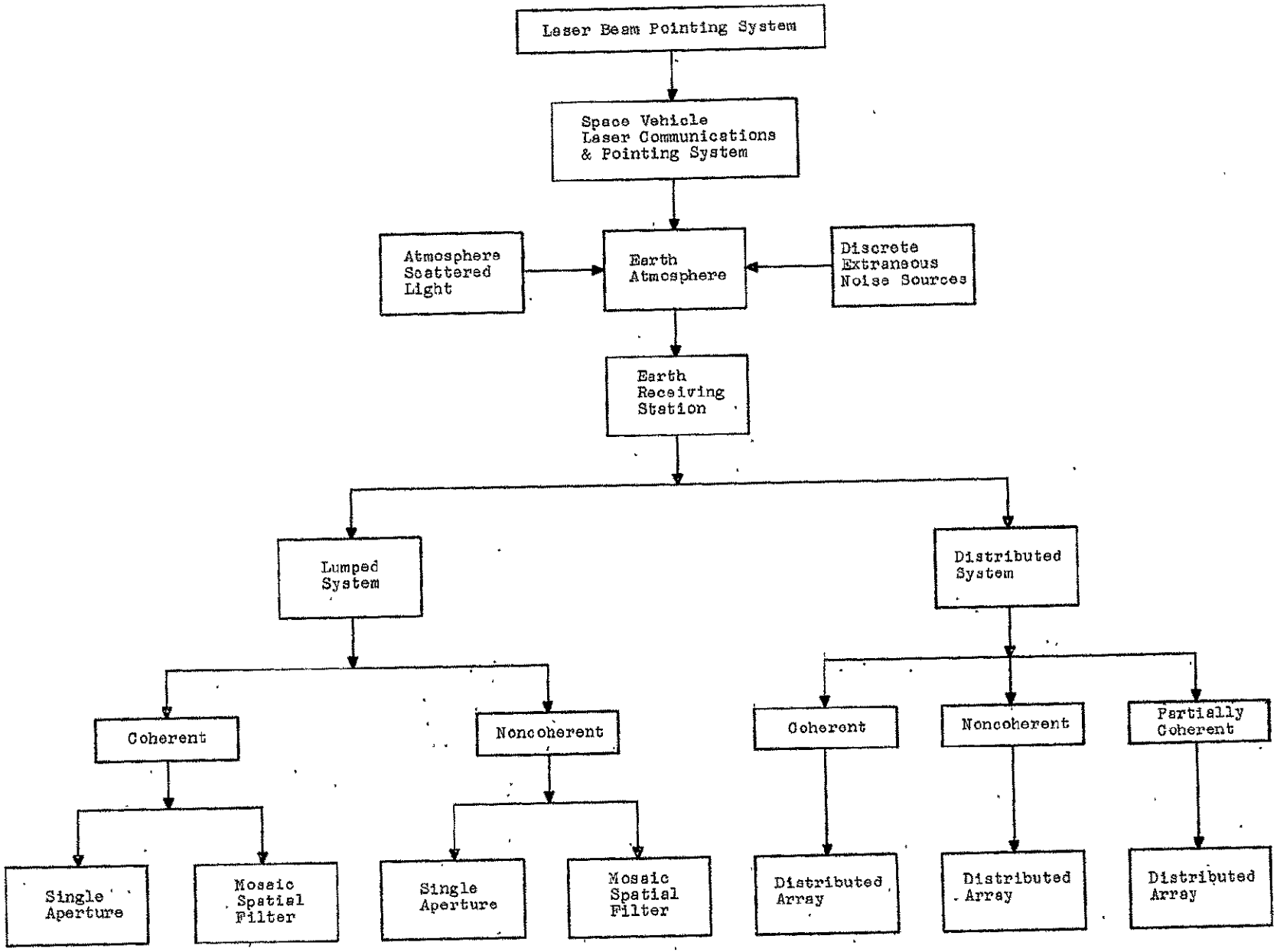

Figure 6. Lumped and Distributed System Configurations

is the conventional mode of a single receiving telescope which can be either a large aperture collector or a phased array, Ref. (19). On the other hand, because it is known that atmospheric degradation and extraneous noise sources represent system problems, local spatial filtering can be implemented in the form of a mosaic pattern recognition array. Here the pattern recognition consists either of a spatial filter or an adaptive array or possibly a more complex statistically adaptive pattern recognition system. For example, a phased array can function either as a single aperture or as an adaptive spatial filter.

The "Distributed System" will have a transfer function designed to match the dispersive properties of the atmosphere and the phase coherence degradation introduced by randam turbulence. Three subclasses are shown reflecting the three possibilities, namely: dispersive atmosphere but coherence is preserved, dispersive atmosphere, completely noncoherent, and dispersive atmosphere, partially coherent. If the atmosphere is non-dispersive, the "Lumped System" should be adequate.

This qualitative system analysis applies not only to the Laser Beam Pointing System but is also applicable to laser communications as well. For the purposes of this study, however, attention will be restricted strictly to the beam pointing problem. However, the results of the further investigation of laser propagation through the atmosphere should prove of interest to the communications study.

G. BEAM POINTING ACQUISITION AND TRACK SEQUENCE

Because of the system errors and uncertainties described in Section II D above, the hybrid open-closed loop acquisition and coarse-fine tracking system represents the best compromise between system complexity and component accuracy, cf. Section IIE, Figure 5. Further insight into the operation of the hybrid system can be gained from a brief review of the operational sequence followed by the Earth station and the space vehicle from "initial launch" to "deep space communications". The procedure is essentially similar to that followed in current NASA DSIF operations, Ref. (2), and those postulated for satellite communications in other studies, Refs. (6), (40).

The communications link including the environment is shown in Figure 7, which is abstracted from Figure 3. The acquisition and track operational sequence is given below in the form of a program with suitable code abbreviations. Detailed system block diagrams are now in preparation together with detailed programs for the operational sequence.

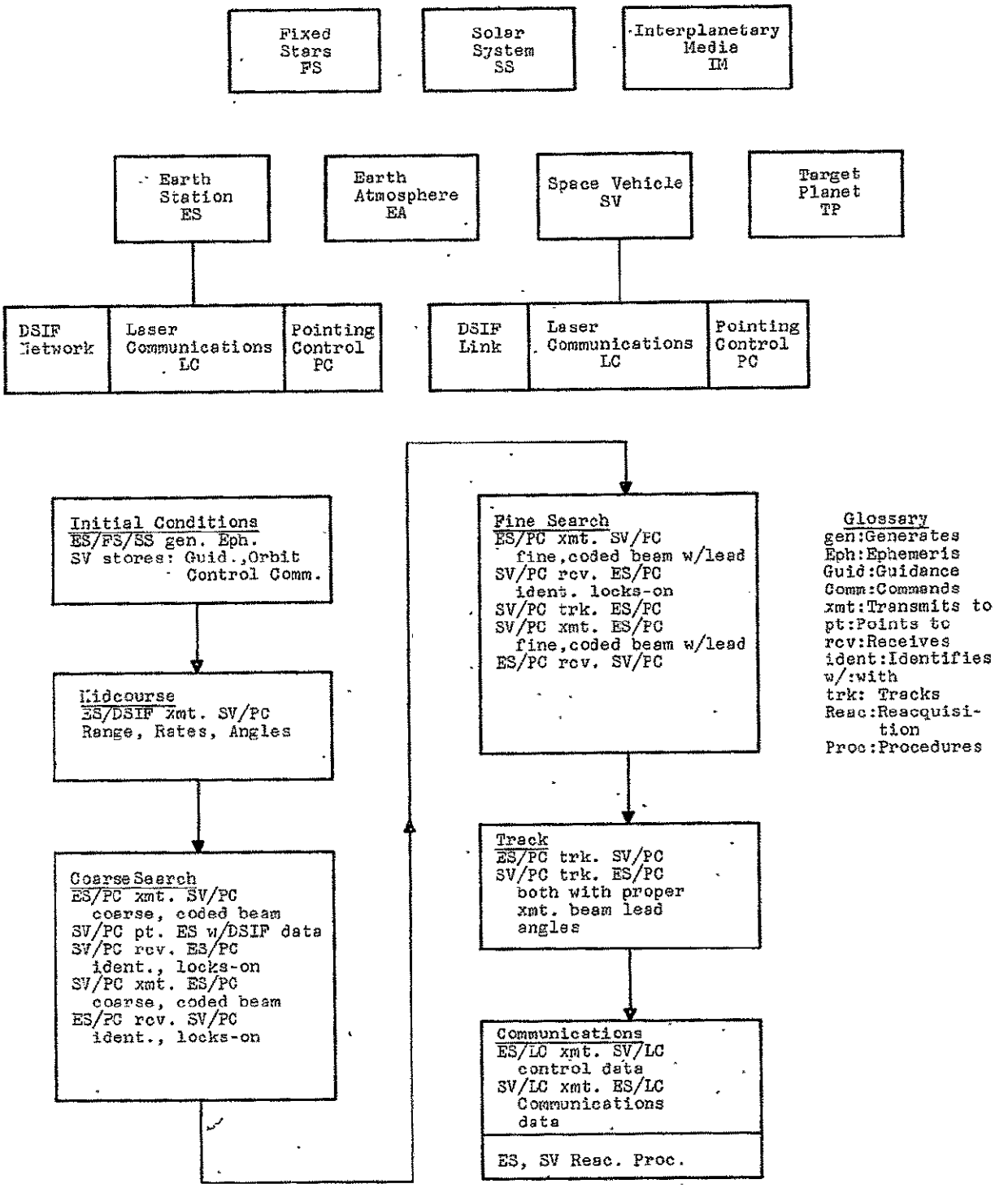

Figure 7. Acquisition and Track Operational Sequence

Essentially, total system operation consists of the four well-known modes: "Search, Detect, Acquire, and Track". The "Track" mode includes closed-loop operation, stabilization (or regulation), smoothing, and lead prediction. The "Search" mode consists of two sequential stages, "Coarse" and "Fine Search". The "Coarse Search" is basically an open-loop process based on DSIF data for both the Earth station and the space vehicle, and in deep space, additional inputs are provided by the celestial and inertial sensors. Once the "Coarse Search" stage is completed, the "Fine Search" stage is a combination open and closed loop process. In the first part, there is a short "Search-Detect-Acquire" sequence within the volume defined by the "Coarse Search" beams. If lead compensation is required for the aberration and transit time effects due to observer and target motion, this is introduced during the "Fine Search" based on the DSIF data. The "Track" mode is cooperative with open-loop lead compensation for the kinematical effects noted above.

In addition to the foregoing, which corresponds precisely to the "In Vacuo" operation described in the preceding section, additional prediction and compensation will be required for the "In Vivo" atmospheric phenomena. The modifications will take place during the "Fine Search" and "Track" modes. Their exact nature will depend on the Earth station system configuration to be selected later in the program.

III. REFERENCE AXES

For both the "In Vacuo" and "In Vivo" cases described in the previous sections, a hybrid open-closed loop beam pointing system is preferred. Suitable "reference axes" must be established within the space vehicle and in the Earth station from which the pointing information for the laser beam is to be derived, cf. Section I A, I B, Tasks 10-15. For the "In Vacuo" case, the obvious sources of reference axis data are celestial sensors and inertial sensors, which function during open-closed loop operation to provide coarse pointing information, and during closed-loop operation to provide stabilization information. During the cooperative phase, the primary reference axis data are provided by the laser beam emanating from the other end of the link.

For the "In Vivo" case, it is recognized that the cooperative laser beam closure is affected by the non-deterministic behavior of the Earth's atmosphere and the interplanetary media. For the narrow beamwidths under study (0.01-1.0 arc second), the random effects of atmospheric turbulence seriously affect the propagation characteristics of the laser beams, albeit differently for each of the two directions of transmission. Because of the crucial nature of these effects on system performance, this section of the report will deal exclusively with laser propagation "in vivo", Section IB, Task 14. Discussions of celestial and inertial data will be presented in the next report.

The following sections present a preliminary analysis of atmospheric phenomena and laser propagation through the atmosphere, with emphasis on the deep space-to-Earth link and direction of transmission. Future reports will cover the direction of propagation from Earth-to-deep space.

A. LASER PROPAGATION AND DIRECTION OF PROPAGATION

It has been well established by various research workers in the field of atmospheric turbulence, Refs. (41) (42), that the effect of atmospheric turbulence on astronomical "seeing" is a serious problem. Turbulence in the atmosphere between a point object and an optical imaging system causes the image of that point object to be degraded in various ways. The image will fluctuate randomly in both intensity, (scintillation), and position, (angle of arrival fluctuations).

Before one tries to apply the large body of knowledge in the area of astronomical "seeing": to the laser beam propagation problem, a significant difference must be pointed out. The laser beam has a wavefront with finite dimensions. This differs from the astronomical case where the wavefront from a star is of infinite extent. In this latter case, there is essentially the same amount of light scattered into the "receiving" beam as there is scattered out, whereas for the finite diameter beam there is a greater loss caused by outward scatter.

It is useful to divide the envisioned modes of laser propagation into separate cases, Ref. (43):

1) Space-to-Earth

2) Earth-to-Space

This division is made since the effects of atmospheric turbulence in each case are of differing nature.

1) Space-to-Earth

The case of laser communications from space to earth is very similar to the astronomical viewing of stars, save for the aforementioned exception. Scintillation, as mentioned earlier is mainly caused by turbulence in the tropopause (15-20 km), and can be characterized by fluctuations in the intensity of starlight. Scintillation seldom exceeds ±25% of the mean value of received intensity and can be suppressed by using larger telescope apertures. The image motion of an extra-terrestrial point source star, which is caused by the thermals close to the earth's surface, will not under certain conditions affect the intensity. More detailed information on this aspect of atmospheric laser propagation will be considered later. The terrestrial receiver telescope detector can be made to receive the entire moving image by adjusting the field of view.

The transmitting telescope aperture size is determined by the pointing ability of the spacecraft. The receiver telescope aperture should be as large as possible commensurate with the economics of the mission contemplated.

2) Earth-to-Space

This mode of propagation can be from an astronomical observatory on earth through the atmosphere to a space station or deep space vehicle. This mode is much more difficult than mode (a) due to the effect of beam scanning or image motion caused by thermals at the site of the transmitting telescope. The space vehicle receiver telescope aperture usually cannot be made large enough to receive the entire beam because of the long ranges involved. Image motion or scanning is the result of thermal pockets in the Fremel zone of the beam which are larger than or approximately equal to the size of the beam. If the telescope aperture is made very large with respect to the size of the thermal pockets, the scanning is reduced to a steady blur. When the scanning of the beam is replaced by the steady beam pattern, a receiver of small angular aperture will not suffer severe modulation. A severe economic engineering problem that must be contended with for this type of system is that a very large transmitting telescope must be of astronomical quality.

A simplified pictorial representation of a deep-space laser communication link is shown in Figure 8. Table VII outlines the major differences between space-to-earth and earth-to-space laser communications as far as the influence of atmospherics is concerned.

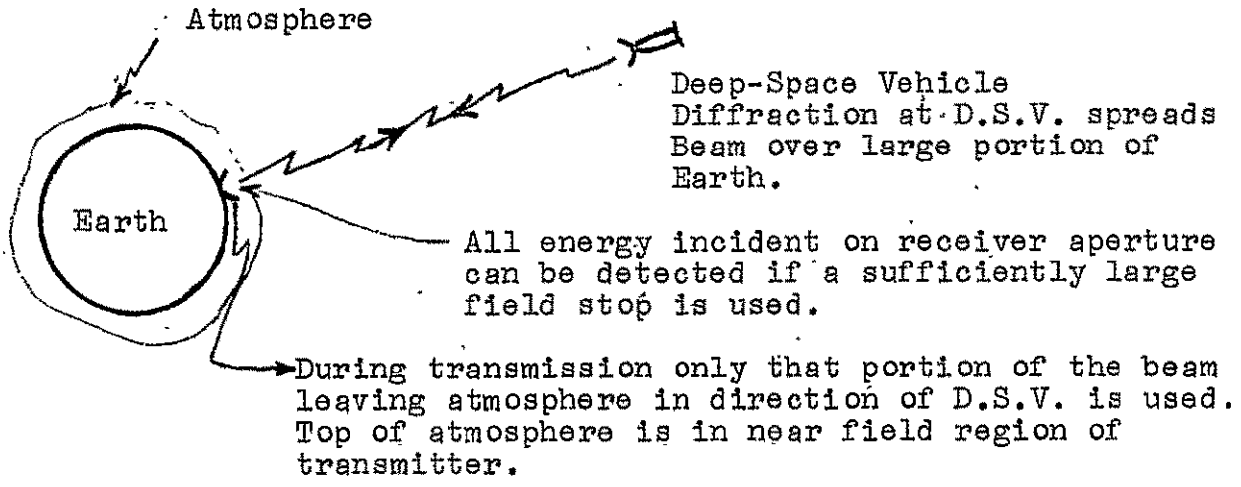

Figure 8. Deep Space Laser Communication Link "In Vivo"

Table VII

Major Difference Between Modes of Simple Laser Deep Space Communication Link

Mode 1: Space-to-Earth

1. Can reduce received intensity fluctuations by using large aperture.
2. Angle of arrival fluctuations caused by thermals near ground do not seriously affect intensity.
3. Receiver telescope detector can be made to receive entire moving image by adjusting field of view.
4. Transmitter telescope aperture size determined by pointing ability of deep-space vehicle.
5. Receiver telescope aperture large as possible to fit economics of mission.

Mode 2: Earth-to-Space

1. This mode is more difficult than mode A due to beam scanning caused by thermals at site of transmitting telescope.
2. Receiver telescope aperture can't be made large enough to receive entire beam because of long ranges involved.
3. Image motion or scanning is result of thermal pockets in Fremel zone of beam which are larger than or approximately equal to size of beam.
4. Large transmitting telescope required must be of astronomical quality if this type of mode is envisioned
5. In transmission, cumulative phase fluctuations (causing angular divergence) are important.
6. In reception only cumulative amplitude fluctuations (produced by phase fluctuations near top of atmosphere) are significant. Fluctuations during reception are much smaller than those during transmission.

An additional complexity must also be given consideration, if special conditions of absolute or relative phase coherence are placed on the laser beam pointing system.

The above considerations apply to a basic laser optical communication link. These concepts must be extended if a more sophisticated tracking and communication complex, (coherent optical phased array), is to be used. Future reports will deal with the propagation limitations on array configurations.

B. ATMOSPHERIC LIGHT PROPAGATION AND BACKGROUND RADIATION

Laser propagation may be studied on the basis of the various atmospheric and interplanetary effects which must be considered. These are:

a) "Seeing" effects, caused by random index of refraction fluctuations of the air.
b) Absorptive attenuation
c) Scattering (non-absorptive attenuation)
d) Background radiation
e) Interplanetary media

Refer to Figure 9 for a factor chart on laser beam propagation.

The first item above will be considered at some length later in this report. Since most pertinent theoretical and experimental information available on refractive effects deal with transmission from outer space (star) to earth, the tracking and communication problem has been modified and attacked along theselines, i.e., transmission from deep-space vehicle to earth. Due to the non-reciprocity of the laser communication link, the present day theory on "seeing" effects must be further modified to allow computation of atmospheric degradation on the reverse link, i.e., earth-to-deep-space. This topic will be dealt with in future reports. An approach shown in schematic form in Figure 10 may be of use in evaluating the performance of an earth laser transmitter system.

1. Atmospheric Attenuation and Scattering, Refs. (44,45)

Scattering and absorbing smoke, smog, dust, salt particules, pollen, haze, and tenuous ice and water droplet clouds are widely distributed throughout the troposphere even when the sky is, meteorologically speaking, clear. Tables of attenuation of visible and infrared radiation under model "clear standard atmospheric" conditions are available, Ref. (44). These tables are useful because of the spectral and altitude ranges covered and the inclusion of realistic aerosol distributions. Both Rayleigh (molecular) and aerosol attenuation coefficients are tabulated. For example, at 0.7μ the Rayleigh coefficient is 8.157×10^{-3} km^{-1} and the aerosol coefficient is 1.50×10^{-1} at the surface level. This is based upon aerosol concentration measurements under or adjusted to conditions when visibility is 20-25 km. Therefore, at least in the lower atmosphere, the clear air attentuation is much more sensitive to particulate than molecular concentration, especially since molecular concentration is relatively constant at any given level.

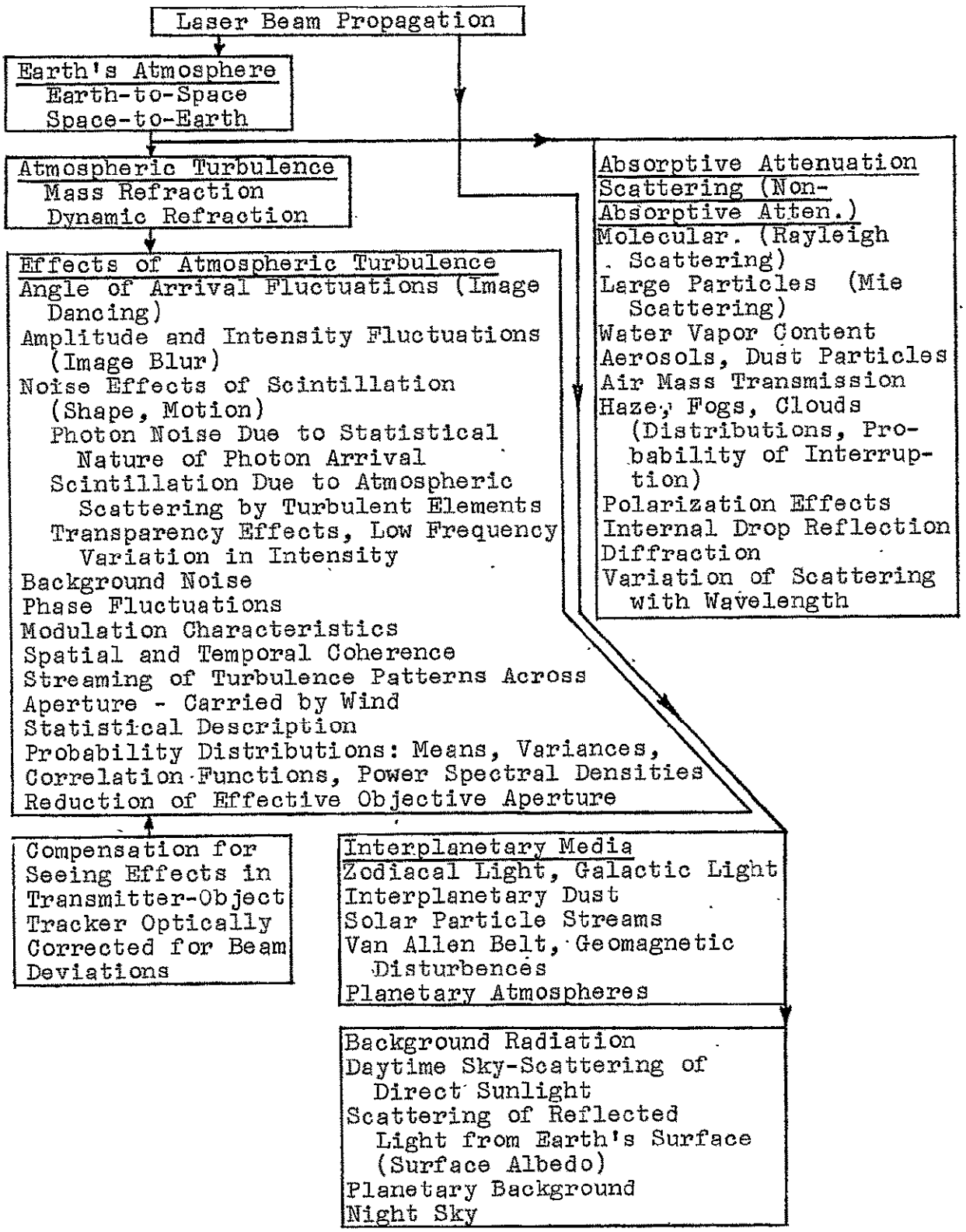

Figure 9. Laser Beam Propagation Factor Chart

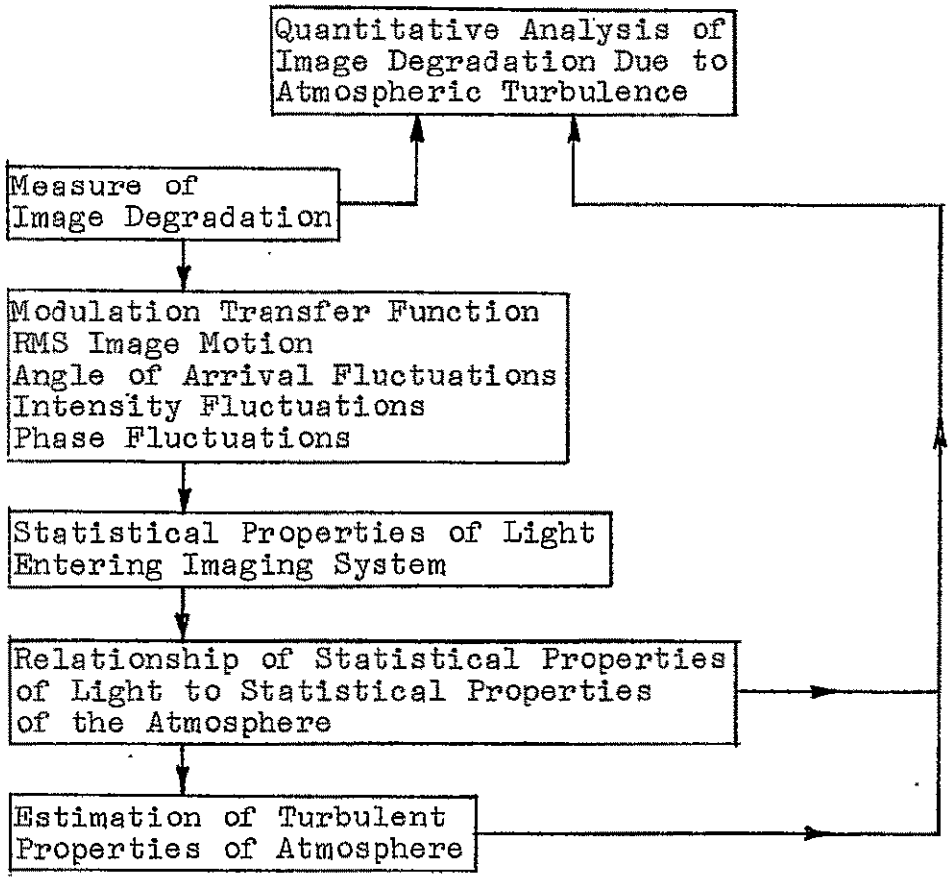

Figure 10. Diagram of Analysis of Image Degradation Due to Atmospheric Turbulence

Long in Ref. (46) has specified gaseous attenuation at ruby laser wavelengths in an analysis of attenuation versus wavelength over the probable operational bandwidth (as controlled by temperature) of this type of laser. Several atmospheric absorption bands due to oxygen and water vapor have been noted, and one strong (55%) absorption line a few tenths of an angstrom wide due to iron in the solar atmosphere lies at about 0.6945 . Ligda in Ref. (44) has suggested that when it becomes possible to construct filters with a bandpass of a fraction of an angstrom, attention may focus on exploitation of this line, with the attendant solar noise reduction.

Transmission through the atmosphere versus wavelength and zenith angle is shown in Table VIII. This information taken from Ref. (47) includes the effects of molecular scattering with vapor ozone absorption, and dust in fairly-clean conditions for a normal atmosphere.

Table VIII

Transmission Through Atmosphere Versus Wavelength and Zenith Angle

Wavelength λ in Angstroms	Zenith Angle in Degrees 90	85	80	60	0
3000	3.16×10^{-75}	3.99×10^{-21}	1.13×10^{-11}	1.23×10^{-4}	.0110
4000	2.58×10^{-8}	8.32×10^{-3}	.0760	.400	.630
5000	1.59×10^{-4}	.0913	.276	.633	.795
6000	2.19×10^{-3}	.166	.382	.710	.844
7000	.0313	.384	.600	.835	.911
8000	.0872	.512	.698	.882	.939
9000	.147	.590	.755	.906	.952
10,000	.336	.650	.794	.923	.961

Clouds and fogs, present the most serious attenuation factors along an extended path. The degradation may even be exceeded by localized dense smoke plumes and dust concentration.

Clouds range tremendously in thickness, and particle concentration. The cloud cover problem must be anticipated for an earth-deep space laser communication system, Refs. (48), (49). The tradeoffs between probability of deep-space-vehicle observability and number of earth receiving stations must be carefully studied from a logistics and economic point of view. Factors such as longitude and latitude of earth sites, annual hours of sunshine, longitude coverage, statistical mean number of days per month that cloud cover over a station is less than or equal to some prescribed threshold must be evaluated for the various contemplated missions. Data from Tiros and Nimbus cloud cover pictures should also provide insight to the problem.

Precipitation away from clouds may not seriously attenuate a laser beam if there is a relatively low concentration of drops per unit volume. Snow probably attenuates more than rain because of the larger particle size and lower forward scattering factor.

2. Sky Background, Ref. (50)

It is possible to classify sky background noise in two ways:

External background noise which may arise from extended sources which fill the receiver beam.

External background noise arising from small sources which do not fill the receiver beam.

It is necessary when considering the above two items to know the magnitude and spectral distribution of flux incident upon the detector from background sources.

For the first case five types of backgrounds should be considered.

a) The Sun
b) Reflected sunlight from:
   i) Moon
   ii) Earth
   iii) Other planets
c) The day sky

For the second case the night sky background should be considered.

a) The Sun

The irradiance of the sun just outside the earth's atmosphere is 1390 watts/ m^2. At the earth's surface the spectral distribution is modified by the transmittance of the atmosphere.

b) Sunlight Reflected from Moon, Earth, and other Planets

The spectral distribution of reflected sunlight is identical to that of sunlight only if the reflectance of the object is independent of wavelength. This appears to be a fair approximation for several cases.

i) Moon

The lunar irradiance of the full moon is approximately 1/465,000 that of the sun, or 3.0×10^{-3} watt/m^2 just outside the earth's atmosphere and its spectrum is essentially the same as sunlight.

The irradiance falls off rapidly as the elongation angle (phase) goes from 180° (full moon) to 0° (new moon). The half moon (90°), though apparently half the area of the full moon is 11% as bright. This rapid fall off is due mostly to the rough character of the surface which causes it to be more or less darkened, except when full, by shadows cast by surface irregularities. The non-uniformities of the surface are an important factor when the receiver's field of view is small.

ii) The Earth

The earth's albedo (reflection coefficient) may be determined from measurements of the earth-shine on the moon, and also from estimates based on individual albedo of ground, sea, forest, snow and clouds. The actual albedo is strongly affected by cloud cover. A value of 0.39 will be assumed. With this value, the irradiance of the full earth at the mean moon distance must be 0.22 watts/m^2.

The spectrum of reflected sunlight from the earth is accentuated in the blue region. This is due to the fact that there is an increased contribution of atmosphere scattering at the shorter wavelength.

iii) Other Planets

The albedo of various planets is presented in Table IX. Venus, the brightest planet seen from the earth, has an irradiance outside the earth's atmosphere of from 0.46 to 1.15 μ watts/m^2.

Table IX

Albedo of Various Planets

Planets	Visual Albedo
Mercury	0.069
Venus	0.59
Mars	0.154
Jupiter	0.56
Saturn	0.63
Uranus	0.73

c) The Day Sky

The day sky will exhibit wide variations in radiance and in spectral content depending upon the sun's position, weather conditions, and receiver orientation.

When the sun is near its zenith on a clear day, the sky is predominantly blue, due to Rayleigh scattering. When the sun is near the horizon, the blue component in the sun's rays is severely attenuated from Rayleigh scattering by the time they reach an area overhead. Rays are now rich in red-yellow portion of the spectrum. Clouds and dust particles illuminated by this light make the sky appear red or yellow in hue.

The flux density per steradian of the receiver's field of view is of the order of 10 to 30 watts/m^2-ster., for a clear day sky.

d) The Night Sky

The spatial distribution of stars has been well documented in the literature. Combining this data with some assumptions on the average spectrum of stars allows a determination in a statistical manner of the effect of this background noise. Refer to Ref. (50) for further details on this source of noise, as well as a summary and description of the phenomena of zodiacal light and galactic light which constitute components of the space background.

C. LASER BEAM ANGLE OF ARRIVAL FLUCTUATIONS

This section will deal with the determination of the angle of arrival fluctuations of the laser beam due to atmospheric turbulence and the dependence of these fluctuations on various system parameters.

Hufnagel in Ref. (51) has shown that the rms one-dimensional position deviations (at the image plane) of the instantaneous center of gravity of the image of a point is given approximately by

$$\sigma \cong \left[\langle s^2(D)\rangle\right]^{1/2} \frac{F}{D} \qquad (1)$$

where $\langle s^2 \rangle$ is a function describing the random optical path length fluctuations between the object and the image forming system

F = focal length of the receiver optical system
D = aperture diameter of the image forming system

The total rms deviation in two dimensions is $\sqrt{2}\,\sigma$

The function $\langle s^2(p)\rangle$ is the mean squared value of the fluctuations of the difference in optical path lengths as measured along straight lines from the object to two points in the entrance pupil which are separated by a distance p. In equation 5.9 of Ref. (52), Hufnagel expresses $\langle s^2(p)\rangle$ in terms of statistics of the intervening index of refraction.

$$\langle s^2(p)\rangle = \int_0^L dz' \int_{-\infty}^{\infty} \left[D_N(r''; z') - D_N(z''; z') \right] dz'' \qquad (2)$$

where $$r'' = \left[p^2 \left(1 - \frac{z'}{L}\right)^2 + (z'')^2 \right]^{1/2}$$

The variable z' is the distance from the imaging system to the object at a distance L.

The atmospheric structure function $D_N(q;z)$ is the mean squared fluctuation of the difference in index of refraction at two points separated a distance q apart at an average distance z from the imaging system. The structure function is related to the correlation ρ between the index fluctuations at the two points by the relation:

$$\rho = 1 - \frac{D_N(q;z')}{D_N(\infty;z')} \tag{3}$$

$D_N(o;z')$ is identically zero.

At this step in the analysis, Hufnagel appeals to the rather large, but still inadequate body of theoretical knowledge and experimental data concerning atmospheric turbulence to evaluate $D_N(q;z')$.

For the q values of interest, D_N is approximately of the form

$$D_N(q;z') = \begin{cases} c_N^2\left[q^{2/3} - \frac{2}{3}l^{2/3}\right] & \text{for } q \gg l \\ \frac{1}{3}c_N^2 q^2 l^{-4/3} & \text{for } q \ll l \end{cases} \tag{4}$$

Where C_N and l are in general both functions of z', and the local meteorological conditions, C_N is called the structure constant, and l, the inner scale length of turbulence. Upon substitution of equation (4) into equation (2) and subsequent numerical integrations one obtains

$$\langle s^2(p)\rangle = 2.91\, p^{5/3}\int_o^L c_N^2(z')\, f\left[\frac{p}{l(z')}\right] dz'$$

$$\text{where } f = \begin{cases} 1 & \text{for } l(z') \ll p \\ 0.92\left(\frac{p}{l}\right)^{1/3} & \text{for } l(z') \gg p \end{cases} \tag{5}$$

This is the case of zenith viewing of a far extra-atmospheric object (plane wave source), $C_N(z') \neq 0$ for $z' \ll L$.

Figures 11 and 12 are plots of the average structure constant and average inner scale length versus altitude, respectively, computed from empirical data. These curves are averages for the conditions stated, and considerable departures may occur in individual situations especially near atmospheric inversion layer boundaries. The rapid decrease in C_N and the rapid increase in ℓ at altitudes above a few kilometers are both caused mostly by the decreased atmospheric density at these elevations.

The following example is presented to show the applicability of the above theory to the determination of the rms stellar image motion for a 30 cm. diameter astronomical telescope under zenith viewing conditions.

A numerical integration of equation (5) for the values of interest and the C_N and ℓ values given in figures 11 and 12 give the result (in cgs units).

$$\langle s^2(\rho) \rangle \cong \begin{cases} 1.7 \times 10^{-10} \rho^{5/3} & , \rho \geq 2\,cm \\ 1.35 \times 10^{-10} \rho^{2} & , \rho < 2\,cm \end{cases} \qquad (6)$$

Substitution into equation (1) for D = 30 cm. gives

$$\frac{\sigma}{F} = \frac{\left[1.7 \times 10^{-10} (30)^{5/3}\right]^{1/2}}{30} = 7 \times 10^{-6}\ \text{radians} = 1.4\ \text{sec.} \qquad (7)$$

This result is in excellent agreement with Hosfeld's photoelectric observations, Ref. (53), with the 31 cm. aperture McMillin Observatory telescope. Hosfeld reports an rms image motion of 1.5 seconds.

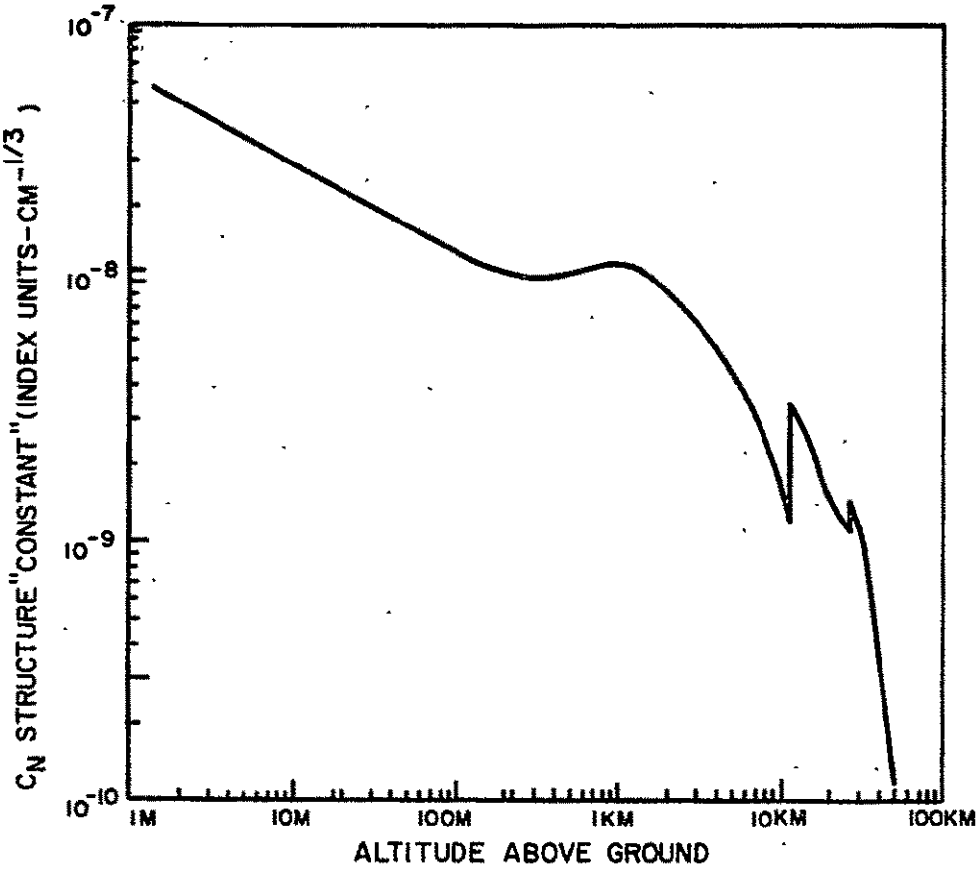

Figure 11. Average Structure Constant vs Altitude, Computed from Empirical Data

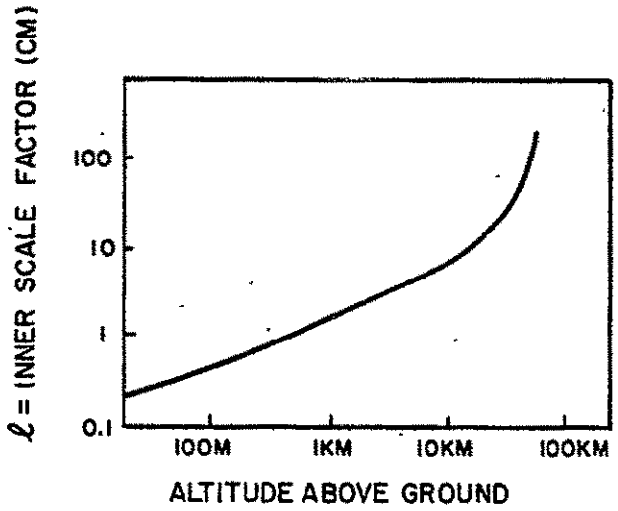

Figure 12. Average Inner Scale Factor vs Altitude, Computed from Empirical Data

For a path through the entire atmosphere at an angle α from zenith (neglecting Earth curvature effect) one has

$$L - z' = h \sec \alpha \qquad (8)$$

Where h is the altitude of the earth based observatory and L is the z-coordinate of the system entrance pupil $\langle s^2(D) \rangle$ can then be expressed as:

$$\langle s^2(D) \rangle = 2.91 D^{5/3} \sec \alpha \int_0^\infty C_N^2 \, dh \qquad (9)$$

The integral $\int_0^\infty C_N^2 \, dh$ has been numerically integrated and is equal to 6×10^{-11} $cm^{1/3}$. Substituting equation (9) into the equation for angle of arrival fluctuations, one obtains

$$\frac{\sigma}{\lambda} \cong \frac{\left[\langle s^2(D) \rangle\right]^{1/2}}{D} = \frac{1.3 \times 10^{-5} \sqrt{\sec \alpha}}{D^{1/6}} \qquad (10)$$

where D in equation (9) and (10) is expressed in centimeters.

Refer to Table X for the rms angular jitter (angle of arrival fluctuations) under average seeing conditions for various zenith angles. It is assumed that diffraction limited optics are employed and the wavelength λ is equal to 6328Å. It is of interest to note that the angular jitter for viewing through the entire atmosphere will be larger than that encountered from mountain top observations, so that the data in Table X are conservative upper bounds. In order to evaluate the angular jitter experienced at mountain top elevations it would be necessary to modify equation (9) by numerically integrating C_N from that elevation to infinity rather than from zero to infinity.

Table X

RMS Angle of Arrival Fluctuations versus Zenith Angle and Receiving Aperture Diameter

Diffraction Limited Beamwidth	1.0	0.1	0.01
Receiving Aperture Diameter (Meters)	0.131	1.31	13.1
Zenith Angle in Degrees	RMS Angular Jitter		(arc-sec)
0	1.75	0.76	0.51
30	1.88	0.82	0.55
45	2.08	0.91	0.61
60	2.45	1.08	0.72

D. ATMOSPHERIC TURBULENCE LIMITATIONS ON GAIN AND DIRECTIVITY

The gain of a laser transmitter is defined as the ratio of the peak illumination produced by the beam in the far field to that of the illumination produced at the same spot by an isotropic radiator. The peak gain of a laser telescope system can be related to the 3 db beamwidth. This may be done by assuming that the radiation emerging from the telescope has approximately the same angular distribution in the far field as would be obtained by diffraction from some uniformly illuminated circular aperture. For this type of aperture the peak gain is

$$G = \frac{4\pi A}{\lambda^2} \qquad (1)$$

where A is the area of the aperture $= \frac{\pi D^2}{4}$ and D is the diameter of the aperture.

The beamwidth θ is related to the diameter of the aperture by the relation

$$\theta = \frac{K\lambda}{D} = \text{directivity} \qquad (2)$$

Therefore the peak gain is equal to

$$G = \left(\frac{\pi K}{\theta}\right)^2 = \left(\frac{\pi D}{\lambda}\right)^2 \qquad (3)$$

Use of present state-of-the-art gas laser and high quality optics have already made possible beamwidths of the order of 2 arc-seconds, Ref. (43). Assuming uniformly illuminated aperture (K = 1.03), the gain of a combined laser telescope system with this beamwidth is 1.5×10^{11}. The gain will be degraded by a factor of two or three due to broadening of directivity by atmospheric seeing disturbances. If a nonuniform illumination pattern is used, further degradation in directivity will be observed. This factor would limit the real gain in a present state-of-the-art laser transmitter telescope system to a value of $G \cong 3 \times 10^{10}$. An increase in aperture size may not improve the gain to any significant degree.

For the Beam Pointer Program, gains of 10^{11} to 10^{15} may be required. From the above considerations, a coherent optical array concept (distributed system) may provide a solution to the limitations imposed by random atmospheric turbulence as previously discussed in Section IIF.

In a free space environment, the gain and directivity are limited only by the optics. For example, the Mount Palomar 200" reflector telescope is accurate to within 1/20th wavelength over the entire surface. In free space this telescope would have a directivity of 1.5×10^{-7} radians or approximately 0.03 arc-seconds, and a gain of 6.25×10^{14}.

E. LASER BEAM INTENSITY FLUCTUATIONS

As mentioned in Section III A, atmospheric turbulence will cause fluctuations in intensity of a received laser beam. The case of transmission from a deep-space vehicle to an earth receiving station is now considered.

For theoretical and experimental investigations, it has been demonstrated that as the diameter of a receiving aperture increases, intensity fluctuations decrease. With a decrease in diameter of a receiving aperture there is a shift of scintillation frequency to higher values.

Scintillation is due primarily to turbulent atmospheric elements at some distance from the observer as opposed to image dancing and pulsation which are due to turbulent elements closer to the observer. From high altitude experimental flights it has been noted that scintillation is highly correlated with winds near the tropopause and that scintillation frequency is a function of wind velocity near the tropopause and turbulence size.

Refer to Figure 13 for a listing of the pertinent atmospheric environmental factors and Figure 14 for a sketch of the turbulent effects encountered at various altitudes above the earth, Ref. (54).

Scintillation is also time of day dependent. A maximum of scintillation occurs at noon; a minimum near sunset and sunrise. A secondary maximum occurs at night which is substantially less than the daytime case. "Seeing" also shows fluctuations with weather systems. The poorest "seeing" usually occurs during cyclone (low) conditions.

Environmental Parameters

Seeing Conditions - Seeing Disc Diameter
Index of Refraction Correlation Function
Atmospheric Structure Function
Inner and Outer Scale Lengths of Turbulence, Shadow Band Pattern
Temperature Gradients
Pressure, Humidity, Air Density
Wind Velocity, Shear, Richardson Number
Season, Time of Day
Observer Altitude
Terrain
Lapse Rate, Gravity Waves

Figure 13. Atmospheric Environmental Factors

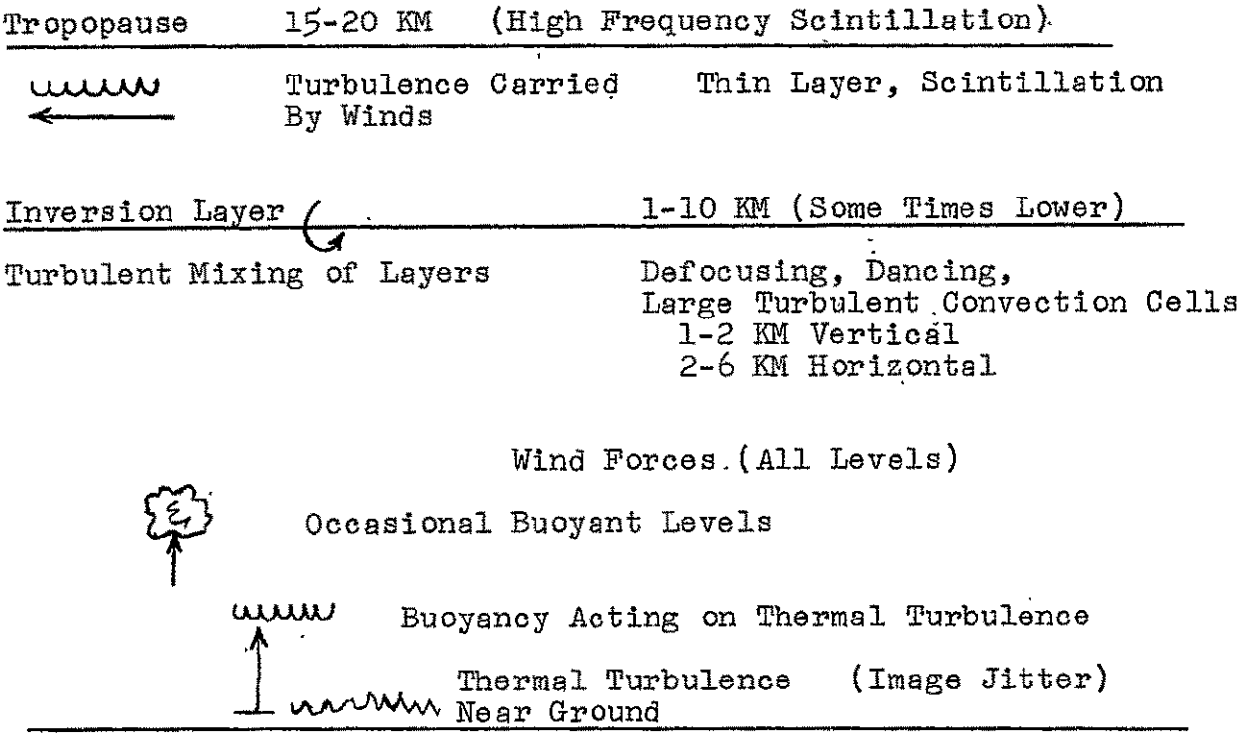

Figure 14. Turbulent Effects Encountered at Various Altitudes

1. Sources of Poor Seeing

The following list of four sources of poor "seeing" will establish the environmental conditions that an earth-based observatory may have to work under.

a) Turbulence caused by convection currents - daytime phenomenon can occur at night in poorly chosen locations.
b) Winds give rise to turbulence near surface of the ground - day or night phenomenon.
c) Strong temperature inversion and motion of air. Wave like turbulence exists at the interface of two air masses.
d) Turbulence caused by air moving past an obstacle such as an observatory dome.

2. R.M.S. Intensity Fluctuations of Received Laser Beam

As stated in Table VII, in the transmission case - from an earth station to a deep-space vehicle, cumulative phase fluctuations which cause angular divergences are important. In reception at the earth station, only the cumulative amplitude fluctuations produced by phase fluctuations near the top of the atmosphere are significant.

The rms intensity fluctuation due to turbulence as a function of zenith angle and receiving aperture have been computed for the case of reception of transmission from a deep-space vehicle.

Tatarski in Ref. (41) has shown that the rms fluctuations in received intensity of starlight can be given by:

$$\left.\frac{P}{P_o}\right]_{rms} = \exp\left[a\, D^{-7/6} \sec^{3/2}\theta\right] \qquad (1)$$

where P is the flux incident on a telescope aperture having a diameter D at a zenith angle θ. Po is the logarithmic time average of P, i.e., $\ln P_o = \overline{\ln P}$; and a is an empirical atmosphere constant $\cong$ 3.16 (daytime conditions).

Table XI gives the rms intensity fluctuations versus the various system parameters of interest. The scintillation will not be appreciable for a large aperture diameter receiver provided the signal strength is made large enough. Various portions of a message could be missed on account of fading if this is not the case, Ref. (48).

Table XI

RMS Intensity Fluctuations versus Zenith Angle and Receiving Aperture Diameter

Receiving Aperture Diameter (Met.)	0.131	1.31	13.1
Zenith Angle (Degrees)	RMS Intensity Fluctuation		$\frac{P}{P_o}$ RMS
0	1.6	1.4	1
30	1.8	1.5	1
45	2.2	1.7	1
60	4.1	2.5	1

F. ATMOSPHERIC TURBULENCE LIMITATIONS ON OPTICAL HETERODYNE RECEPTION

It was previously indicated in Section II F that "In Vivo" operation gives rise to conflicting constraints on the Beam Pointing System in terms of extraneous noise sources on the one hand, and the effects of atmospheric turbulence on the other. The former constraint leads to the conclusion that narrow bandwidth optical heterodyne reception is desirable. The latter constraint dictates the use of layer telescope receiving apertures to reduce "image dancing" and "scintillation". These conclusions are in opposition as the following sections will demonstrate. Hence it was further concluded in Section II F that "distributed" systems should be considered as well as "lumped" systems in order to mediate the opposing requirements.

A principal reason heterodyne reception is desirable is that it should permit narrow-band, photon-noise-limited operation with solid-state detectors. The quantum efficiency of these detectors is higher than that attainable with photoemissive surfaces, and therefore the required signal power might be substantially reduced. At a wavelength of 6300Å, the quantum efficiency of a silicon photodiode is approximately 0.5 whereas the quantum efficiency for a tri-alkali photosurface is 0.05.

For an earth-based system, heterodyne detection of transmission from a deep-space vehicle becomes difficult for large receiver telescope apertures. This is because there exist random phase differences among the light wave fronts in various parts of the telescope aperture due to atmospheric turbulence. Heterodyne reception depends upon phase coherence between the local oscillator and the signal, and it is difficult to compensate for a multitude of different phases across the aperture. The heterodyne detector system as illustrated in Figure 15 converts a steady signal into a much weaker and noisier signal because the voltage due to various portions of the wave front would add and subtract randomly. Also,even assuming a uniform wave front, there is the problem of generating a constant-amplitude local oscillator signal. This, however, is strictly a technical problem which will eventually be solved in its own right.

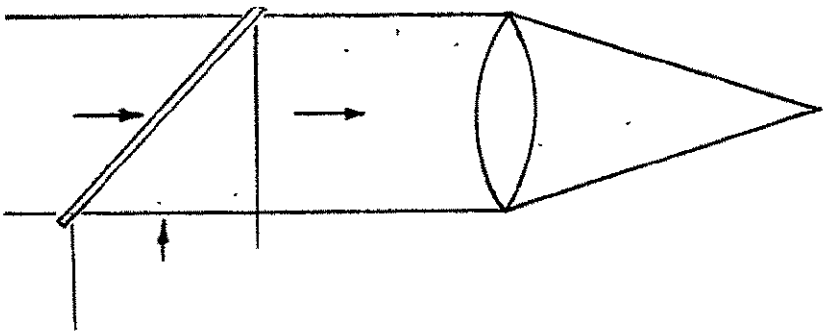

Figure 15. Optical Heterodyne Detection

1. Optical Heterodyne Reception

Similar to the microwave case, an optical heterodyne receiver provides a signal amplitude proportional to the integral of electric field over the aperture. Consequently the aforementioned random spatial variation in amplitude and phase will reduce the received signal power. Following an analytical approach by Gardner, Ref. (55), Fried and Cloud, Ref. (56), the average loss in signal power caused by atmospheric turbulence is determined for an optical heterodyne receiver. Analytical results are obtained in terms of the statistical properties of atmospheric refractive index, wavelength, size of receiving aperture.

Refractive index fluctuations as a result of random temperature variations give rise to amplitude and phase fluctuations in a received optical signal. For an optical heterodyne communication system, the received signal level depends upon phase coherence over the receiving aperture. The random variations in amplitude have been previously assessed in Ref. (41) and these fluctuations can be shown to be less effective than random spatial variations in phase over the aperture.

Referring to Figure 15, E_S represents the signal field and E_{LO} the field produced by the local oscillator. At the lens, the field is:

$$E_T = E_{LO} + E_S \tag{1}$$

At the detector the field E_D can be represented in terms of rectangular coordinates (η, ξ) whose origin is located at the center of the detector.

$$E_D(\eta, \xi) = \int_{LENS} E_T f(\eta, \xi)\, dA_L \tag{2}$$

The function $f(\eta, \xi)$ is approximately a two dimensional Fourier kernel which depends upon coordinates in the aperture plane, and A_L is the area of the receiving lens.

The detector output current is

$$I_D \propto \int_{DETECTOR} E_D E_D^*\, dA_D \tag{3}$$

where * denotes complex conjugate, and A_D is the area of the detector. The current I_D can then be expressed as:

$$I_D \propto \int_{DETECTOR} dA_D \left[\int_{LENS} E_T f\, dA_L\right]\left[\int_{LENS} E_T^* f^*\, dA_L\right] \tag{4}$$

Assuming that the local oscillator component is much larger than the received signal, the signal component in the output current is:

$$I_S \propto \int_{DETECTOR} dA_D \left[\int_{LENS} E_S f\, dA_L\right]\left[\int_{LENS} E_{LO}^* f^*\, dA_L\right] \tag{5}$$

The spatial variation of the last factor in the right hand side of equation (5) in the plane of the detector will consist of a diffraction limited spot, while that of $\int_{LENS} E_s f \, dA_L$ will become much broader due to phase fluctuations.

As a first approximation the signal component is:

$$I_s \propto \int_{LENS} E_s \, dA_L \qquad (6)$$

Therefore, the average signal power received is

$$P_s = \langle I_s I_s^* \rangle = \alpha \left\langle \int_{LENS} E_s \, dA_L \int_{LENS} E_s^* \, dA_L \right\rangle \qquad (7)$$

where α is a dimensionless factor and the brackets denote ensemble average.

When one considers the case where a detector of the same size as the lens is used in place of the lens the signal component can be shown to be equal to, Ref. (55):

$$I_s \propto \int_{DETECTOR} E_s \, dA_D \qquad (8)$$

This result is identical with that obtained in equation (6).

2. Loss in Signal Power Due to Atmospheric Turbulence

Due to temperature stratification with height, there will be spatial variations in average refractive index. Gardner in Ref. (55) considers the case where the receiver is adjusted so that the pointing angle follows the long term variations, but does not appreciably follow the instantaneous angle of the center of the "dancing" image.

The amplitude of the monochromatic light incident normally on a circular aperture of radius R may be expressed as exp $[i\phi(r,\theta)]$, where r, θ are polar coordinates in the aperture plane. The harmonic time dependence has been suppressed and amplitude fluctuation effects are assumed to be of second order.

Gardner shows that the output signal power is:

$$P = \alpha \int_0^{2\pi} d\theta_1 \int_0^R r_1\, dr_1 \int_0^{2\pi} d\theta_2 \int_0^R r_2\, dr_2 \left\langle \cos\left[\varphi(r_1, \theta_1) - \varphi(r_2, \theta_2)\right] \right\rangle \qquad (9)$$

The power loss factor γ defined as the ratio of the actual received signal power to the power which would be measured if phase fluctuations were absent is introduced at this point.

$$\gamma = \frac{1}{\pi^2 R^4} \int_0^{2\pi} d\theta_1 \int_0^R r_1\, dr_1 \int_0^{2\pi} d\theta_2 \int_0^R r_2\, dr_2 \left\langle \cos\left[\varphi(r_1, \theta_1) - \varphi(r_2, \theta_2)\right] \right\rangle \qquad (10)$$

At this stage of the analysis, Gardner assumes that the phase fluctuations are homogenous and isotropic in the plane of the aperture, and possess a joint gaussian probability density. The joint density for the phases $\varphi_1 = \varphi_1(r_1, \theta_1)$, $\varphi_2 = \varphi_2(r_2, \theta_2)$ is:

$$p(\varphi_1, \varphi_2) = \frac{\left[1 - \rho_\varphi^2\right]^{-1/2}}{2\pi \langle \varphi^2 \rangle} \exp\left[- \frac{\left[\varphi_1^2 + \varphi_2^2 - 2\varphi_1 \varphi_2 \rho\right]}{2\left[1 - \rho_\varphi^2\right] \langle \varphi^2 \rangle} \right] \qquad (11)$$

where the phase correlation coefficient ρ_φ is equal to $\frac{\langle \varphi_1 \varphi_2 \rangle}{\langle \varphi^2 \rangle}$ and $\langle \varphi^2 \rangle$ is the mean square phase fluctuation.

The ensemble average of $\cos(\varphi_1 - \varphi_2)$ in the loss factor γ is equal to $\exp\left[-\langle \varphi^2 \rangle (1 - \rho_\varphi)\right]$. The argument of this exponential may be expressed in terms of the so-called "structure function" of the phase fluctuations, since for homogenous and isotropic fluctuations the structure function is related to the correlation function by:

$$D_\varphi(r) = 2\langle \varphi^2 \rangle (1 - \rho_\varphi) \qquad (12)$$

In general the structure function of a locally isotropic random field depends only on the magnitude of the difference of two field points r_1 and r_2. Therefore:

$$D_\varphi(r) = \left\langle \left[\varphi(r + r_1) - \varphi(r_1)\right]^2 \right\rangle \qquad (13)$$

The latter equation can be easily manipulated into equation (12).

The loss factor γ can be obtained by combining the expression for $\langle \cos(\varphi_1 - \varphi_2) \rangle$ and equation (12). Then

$$\gamma = \frac{1}{\pi^2} \int_0^{2\pi} d\theta_1 \int_0^{2\pi} d\theta_2 \int_0^1 x_1 \, dx_1 \int_0^1 x_2 \, dx_2 \exp\left[- D_\varphi\left(\frac{x R}{2}\right)\right] \qquad (14)$$

where $x_1 = r_1/R$ is a non-dimensional length, and $x = |\vec{x_1} - \vec{x_2}|$ the magnitude of a vector difference.

To evaluate the average power loss information is required on the specific form of $D_\varphi(r)$ for separations less than or equal to the diameter, 2R, of the receiving aperture.

Equation (14) may be regarded as a two-dimensional convolution integral. By means of a Hankel transform, Gardner manipulates equation (14) into:

$$\gamma = 4 \int_0^\infty dk \; h(k) \frac{J_1^2(k)}{k} \qquad (15)$$

where

$$h(k) = \int_0^\infty x \, dx \, J_0(kx) \exp\left[- \frac{D_\varphi(xR)}{2} \right] \qquad (16)$$

The dimensionless dummy variable k in equations (15) and (16) is related to the corresponding dimensionless wave number, say k', by $k = k'R$.

At this stage of the analysis in Ref. (55), a result of Tatarski, Ref. (41), is utilized for the phase structure function for horizontal line-of-sight transmission above the earth over a specified range. We will depart from this case to consider laser transmission at a wavelength of 6328A from a deep space vehicle. Vertical downward transmission through the atmosphere to an earth receiving station is analyzed.

Fried and Cloud, Ref. (56), starting from a scalar version of Maxwell's equation in a turbulent medium, solved the equation which then led to a determination of the phase and amplitude fluctuations. The correlation functions for phase and logarithm of the amplitude of a monochromatic plane wave traveling downward through the atmosphere have also been obtained analytically. The solutions are based on Ryter's method for propagation in an inhomogenous medium and Kolmogoroff's theory of correlation in a turbulent fluid, Refs. (41), (42). Various experimental measurements of atmospheric turbulence have also been collected to pro-

vide the data for an analytical model.

For a monochromatic wave with wavelength $\lambda = 6328\text{Å}$, traveling vertically downward through the atmosphere, the structure function for the phase fluctuations was found to be approximately equal to, Ref. (56):

$$D_\phi(r) \cong 910\, r^{5/3} \tag{17}$$

To simplify the computation of the power loss γ, r^2 will be used in the structure function instead of $r^{5/3}$, since r^2 does not differ by very much from $r^{5/3}$.

Substituting $D_\phi(r) \cong 910\, r^2$ into equation (16) and performing the necessary integration one obtains, Ref. (51):

$$h(k) = \frac{1}{910 R^2} \exp\left[-\frac{k^2}{1820 R^2}\right] \tag{18}$$

Now substituting $h(k)$ into equation (15), the power loss factor γ becomes

$$\gamma = \frac{4}{910 R^2} \int_0^\infty \frac{dk\, J_1^2(k)}{k} \exp\left[-\frac{k^2}{1820 R^2}\right] \tag{19}$$

This equation has been numerically integrated. The signal power loss in db is shown in Figure 16 as a function of receiving aperture diameter. For $\sqrt{910}\, R \gg 1$, the loss factor is

$$\gamma \sim \frac{1}{455 R^2} \tag{20}$$

Due to restrictions upon the phase structure function, the above results will be valid only if the diameter of the receiving aperture is much less than the outer scale of turbulence. The outer scale of turbulence is the range in which the index of refraction correlation function decays to half of its zero range value.

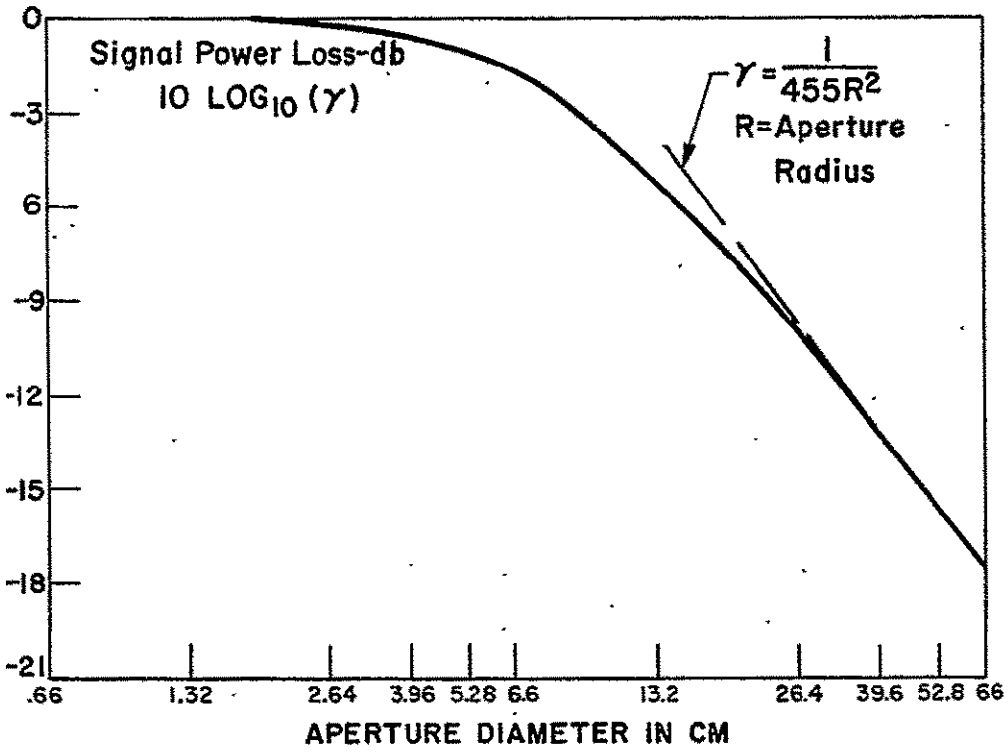

Figure 16. Signal Power Loss Vs. Aperture Diameter for a Vertical Downward Path, With $\lambda = 6328A$

$$\gamma = \text{Power Loss Factor} = \frac{\text{Actual Rcvd. Power}}{\text{Rcvd. Power with no Phase Fluctuations}}$$

The results presented above tend to be in good agreement with that based on typical astronomical resolution. For the astronomical case, a diameter of 10 to 15 cm. is the point for which diffraction-limited resolution approximates atmospherically.. limited resolution.

It if of interest to note that Fried and Cloud, Ref. (56), have suggested that if the local oscillator wavefront in an optical heterodyne detection system could be made to track the average tilt of the distorted wavefront, efficiency of heterodyne reception could be made to saturate at larger receiving aperture diameters than predicted.

The average signal power loss computed above neglects all effects caused by motion of transmitter and receiver. Therefore a calculation of average signal power loss based upon this static model represents an optimistic estimate since any motion can only result in further loss of signal information. Also zenith angle dependence must be taken into account to evaluate performance under slant path conditions.

IV. BEAM MEASURING AND POSITIONING

In the discussion of general considerations of the Beam Pointing System, Section II E, it was concluded that fine beam positioning or beam steering control was required, Section II E, Figure 4. This conclusion has also been reached in other studies, Refs. (6), (19), (31). Because the fine beam deflection is principally employed in the aberration and transit time compensation (lead prediction) subsystem, which is essentially an open-loop process in its simplest approach (Section II E), its linearity, accuracy, and stability requirements are very high. (However, the possibility of enclosing this subsystem within a feedback loop exists and is being investigated).

The following two subsections are devoted to discussions of the general principles of laser beam steering and possible specific phenomena which are currently being exploited or else have potential for this application.

A. GENERAL PRINCIPLES OF OPTICAL BEAM DEVIATION

The deviation or steering of a light beam can be achieved by a) sending the beam through a medium in which the index of refraction has been changed, the refraction approach, b) rotation of a reflecting mirror, reflecting approach, c) diffraction.

1. Refraction

The principle on which the refraction approach is based is the following: A beam of light crossing a boundary between two media of different indexes of refraction, will be deviated from the incident direction. The deviation is proportional to the ratio of the indexes of refraction of the two media.

If we indicate with $\varphi_0, n_0, \varphi_1, n_1$, respectively the angle which the beam direction make with the normal and the index of refraction of the incident and refracted medium, from the law of refraction, we have

$$\varphi_1 = \sin^{-1}\left[\frac{n_0}{n_1}\sin\varphi_0\right] \qquad (1)$$

that is, for a given angle of incidence, φ_0, and index of refraction, n_0, any variation in n_1 will produce a variation in the angle of refraction, φ_1.

From the law of refraction

$$(n_1 + \Delta n_1) \sin(\varphi_1 + \Delta\varphi_1) = n_0 \sin\varphi_0 \qquad (2)$$

$$(n_1 + \Delta n_1)(\sin\varphi_1 + \Delta\varphi_1 \cos\varphi_1) = n_0 \sin\varphi_0 \qquad (3)$$

where we have assumed

$$\lim_{\Delta\varphi_1 \to 0} \sin\Delta\varphi_1 \longrightarrow \Delta\varphi_1$$

$$\lim_{\Delta\varphi_1 \to 0} \cos\Delta\varphi_1 \longrightarrow 1$$

From eq. (3), we have

$$\Delta\varphi_1 = \frac{1}{\cos\varphi_1}\left[\frac{n_0 \sin\varphi_0}{n_1 + \Delta n_1} - \sin\varphi_1\right] \qquad (4)$$

But

$$\sin\varphi_1 = \frac{n_0 \sin\varphi_0}{n_1}$$

$$\cos\varphi_1 = \left[1 - \frac{n_0^2 \sin^2\varphi_0}{n_1^2}\right]^{1/2}$$

substituting in eq. (4), we have

$$\Delta\varphi_1 = \frac{n_1 n_0 \sin\varphi_0}{\left[n_1^2 - n_0^2 \sin^2\varphi_0\right]^{1/2}}\left[\frac{1}{n_1 + \Delta n_1} - \frac{1}{n_1}\right] \qquad (5)$$

$$\frac{1}{n_1 + \Delta n_1} = \frac{n_1 - \Delta n_1}{n_1^2 - \Delta^2 n_1}$$

But $\Delta^2 n_1$ is of the order of 10^{-10} or smaller, so can be neglected respect to n_1^2.

Substituting in eq. (4) and simplifying we obtain

$$\Delta\varphi_1 = \frac{n_0 \sin\varphi_0}{n_1\left[(n_1^2 - n_0^2 \sin^2\varphi_0)^{1/2}\right]}\,\Delta n_1 \qquad (6)$$

The light refracted will have a phase different from the one of the incident light.

For a medium of a given thickness and for a fixed angle of incidence, the phase variation of the refracted light is function of the index of refraction of the medium, i.e., any change in index of refraction will produce a change in the phase of the output light.

Let us suppose a beam of light going through a medium, as in Figure 17.

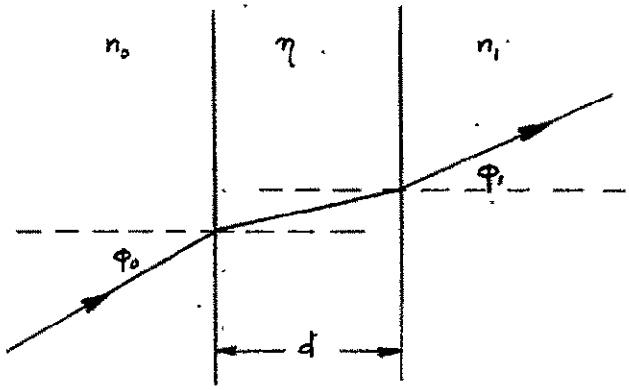

Figure 17. Optical Refraction

For a given thickness, d, and index of refraction, real or complex (the medium is dielectric or absorbing) η, and for wavelength λ, a medium can be represented by a two-by-two matrix of the type

$$\begin{bmatrix} \cos\theta & \frac{i\sin\theta}{\eta} \\ i\eta\sin\theta & \cos\theta \end{bmatrix} \qquad (7)$$

where

$$\theta = \frac{2\pi}{\lambda}\,\eta\, d\cos\varphi_0$$

Using the elements of the matrix, the amplitude transmittance is derived

$$T = \frac{2n_0}{(n_0 + n_1)\cos\theta + i\left(\frac{n_0 n_1}{\eta} + \eta\right)\sin\theta} \tag{8}$$

or

$$T = A - iB \tag{9}$$

where

$$A = \frac{2n_0(n_0 + n_1)\cos\theta}{\left[(n_0 + n_1)\cos\theta\right]^2 + \left[\left(\frac{n_0 n_1}{\eta} + \eta\right)\sin\theta\right]^2}$$

and

$$B = \frac{2n_0\left(\frac{n_0 n_1}{\eta} + \eta\right)\sin\theta}{\left[(n_0 + n_1)\cos\theta\right]^2 + \left[\left(\frac{n_0 n_1}{\eta} + \eta\right)\sin\theta\right]^2}$$

Equation (9) can be put

$$T = A - iB = \rho e^{-i\psi} \tag{10}$$

from which we derive

$$\rho = \left[A^2 + B^2\right]^{1/2} \tag{11}$$

and

$$\psi = \cos^{-1}\left[\frac{A}{(A^2 + B^2)^{1/2}}\right] \tag{12}$$

From equation (6) it appears that if the substrate is known and so the thickness of the medium and the wavelengths of the light, the phase is function only of the index of refraction of the medium.

2. Reflection

In the reflection approach, the beam direction is changed by means of a tilting mirror. The principle is based to the law of reflection of a light beam. The angle of incidence is equal to angle of reflection. By rotating the mirror, the angle of incidence is changed, therefore the angle of reflection is changed.

3. Diffraction

In the diffraction approach, the beam direction is changed by electronically controlling the frequency of an optical grating which is achieved by means of ultrasonic waves set up in a liquid or solid.

It is inefficient to steer a beam using this phenomenon because a) the major signal energy is contained in the zero order diffraction pattern, which does not scan as the grating frequency is changed, b) the secondary orders of the diffraction pattern which do scan as the frequency is varied, are modulated at twice the ultrasonic frequency (for standing waves in the medium).

Techniques based on the principles of refraction and reflection will be discussed in the next section.

B. EXAMPLES OF BEAM STEERING TECHNIQUES

The previous section discussed the principles on which the steering techniques are based. It was noted that the diffraction principle is not efficient for use in beam steering. Therefore we will consider the techniques which make use of the principles of refraction and reflection.

Beam steering using the refraction principle, which changes the beam direction by means of change in refractive index which is induced by means of an applied field or an applied pressure, makes use of the following effects, Refs. (6), (31), (58), (59):

a) Kerr Effect
b) Pockels Effect
c) Variable Density Effect
d) Photoelastic Effect
e) Ferroelectric Effect

The technique which makes use of the reflection principle, that is the technique which changes the beam direction by means of tilting mirror, make use of the Shear Strain Effect.

In Table XII are listed the Effects, their sensitivities and ranges. Table XIII summarizes their advantages and disadvantages.

Table XII

Performance Characteristics of Beam Steering Techniques

Effect	Medium	Sensitivity	Control	Range (1)
Kerr	Nitrobenzine	$1.6(10^{-14})^{rad}/(V/cm)^2$	1-40 Kv/cm	0.025
Pockels	KDP (20°C)	$7.5(10^{-9})^{rad}/(V/cm)$	±40 Kv/cm	0.6
Pockels	KDP (-100°C)	$2.3(10^{-7})^{rad}/(V/cm)$	±40 Kv/cm	18
Ferro Electric	$BaTiO_3$ Crystal ($\leq$ 130°C)	$2.5(10^{-6})^{rad}/CV/cm)$	15±5 Kv/cm	25
Density	CS_2 (Gas)	$1.8(10^{-3})^{rad}/atm$	1±1 atm	3.6
Density	CS_2 (Liquid)	$1.5(10^{-4})^{rad}/atm$	10±10 atm	3.0
Photo Elastic	Glass	$2.0(10^{-6})^{rad}/atm$	100±100atm	0.4
Shear Strain	$BaTiO_3$ (Ceramic)	$6.0(10^{-8})^{rad}/(V/cm)$	±40 Kv/cm	4.8

Note: (1) The units of Range are milliradians

Table XIII

Advantages and Disadvantages of Beam Steering Techniques

Effect	Advantages	Disadvantages	Notes
Kerr	Large cell may be constructed Short Risetime Wide Angular aperture	Small variations in index of refraction-100 v/mil, approx. 2.8×10^{-5} (28 N units). The liquid tends to decompose when in contact with foreign material, heat, high electric field. High voltages.	Electrically induced birefringence in a medium.
Pockels	Change in index of refraction for 100 V/mil appr. 1.4×10^{-4} (140 N units). Linearly proportional to the electric field. Minimum prism deviation would be capable of scanning about 1 min. of arc at room temperature. An increase by a factor of 30 is expected when properly cooled.	Difficulty to shape and polish the crystal. The phosphates used are soluble in water and must be protected from moisture. The crystals are very sensitive to thermal stress when heated or cooled to rapidly. Pair of prisms must be used to cancel the effect of temperature coefficient on the index of refraction.	Direct effect of an electric field on the optical properties of a Piezo-electric crystal.
Variable Density	Gases have height compressibility-A variation of the order of 10^{-3} in refractive index for atm. can be expected.	Liquids have a small compressibility and therefore the maximum change in index of refraction for atm. is of the order of 10^{-4}. Electrical control of pressure with reasonable response speed is difficult or impossible to achieve.	

- Cont'd. -

Table XIII (Cont'd.)

Effect	Advantages	Disadvantages	Notes
Photo elastic	Glass can support compressive stress of 1000 atm. very low power requirements	Change of about 10^{-6} (1 N units) for atm. Difficulty in generating high stress by electrical means.	Change in the optical properties of a crystal when a strain is applied. An electrical field is often used to produce the strain.
Ferro electric			Though potentially good is still under study.
Shear Strain	Shear strain produced in a Barium Titanate Crystal by 100 V/mil give about 10^{-3} radians.		The beam deviation produced by reflection from the deflected surface of such a crystal would be about 7 m' of arc.

The previous techniques are capable of beam deflection of the order of minutes of arc at normal conditions. At low temperatures, around -100°C, may extend this capability to one degree of arc.

One way to obtain this is by multiple reflections between a reference surface and a moving one.

By increasing the angle between the two surfaces, the deflection angle can be increased. The magnification is function of the angle between the two surfaces and the number of internal reflections.

The exit beam will rotate through an angle

$$D = 2(N\beta - M\delta) \qquad (1)$$

where

N = number of reflections from moving surface
M = number of reflections from reference surface
β = angle of rotation of moving surface
δ = angle of rotation of reference surface

The limitations to the number of internal reflections are imposed by the size of the two surfaces and by the loss in light intensity.

Another way to obtain angular magnification is by multiple refractions, applicable to those beam steering devices employing solid prisms. It consists in sending light through a chain of prisms or through a prism several times. The maximum exit beam rotation is probably limited to ±10 degrees.

One of the characteristics that a beam steering device must satisfy is fast response, especially important in the beam pointing system.

Many optical beam steering techniques utilize piezoelectric materials for producing mechanical displacement or stress. In these cases, the response speed could be limited by the electrical impedance of the material and that of the electrodes and leads, and by incapability of the transducer to produce displacements at frequencies above the mechanical resonance frequency.

Sources of errors for the beam steering techniques arise when the system environment is changed. Temperature change, mirrors or lens system misalignment due to shock and acceleration are some of the reasons. The temperature change will produce change in the index of refraction, in the optical path and in the focal length of the lenses.

This negative effect can be reduced by using a thermistor or similar sensor to correct the deflection. The misalignment will produce larger aberrations with the result of decreasing the overall resolving power.

Beside these sources of errors, there are a large number of random and progressive errors which affect the amplitude and (or) the phase, such as:

a) Amplitude error due to the change in reflectivity at interface of two media due to temperature change.
b) Random phase error due to the change in thickness and refractive index of lens material with temperature.

There are, of course, a number of optical losses due to: surface reflection, internal absorption, internal scattering, mirror reflection, interference filter, etc. Many of these losses can be reduced by, for example, properly coating the lenses surfaces, mirrors, etc.

The beam steering is evidently a very involved problem. Many parameters must be controlled to obtain a workable system.

Among the techniques listed, the one making use of the Pockels effect seems very promising. Using this technique, a device has been developed that is temperature independent, Ref. (31). A beam deflection of 30 spot diameters has been obtained, and the device produces modulation as a function of the driving voltage.

V. BORESIGHT MAINTENANCE

A. KOLLSMAN BORESIGHT MAINTENANCE TECHNIQUES

In consideration of Kollsman's long association with the state-of-the-art in the relating of optical lines of sight to most of the standard reference systems, it is important to review some of these proven techniques of establishing, maintaining, and monitoring these boresight relationships.

Boresight stability or maintenance is important to all of the modern, astronavigation instruments in whose evolution Kollsman has played a historical role. The earliest astro-trackers with their "minutes-of-arc" accuracies could rely on the stability of the mechanical and structural design to stay within the boresight deviation tolerance.

Today, the latest versions of these astronavigation instruments are approaching accuracy requirements where seconds of arc have the same significance that minutes of arc had to the earlier instruments of ten years ago. Hence, boresight maintenance and monitoring techniques with their accessory components and subsystems have had to evolve rapidly to meet the needs of the state-of-the-art in pointing at the stars.

The use of the term boresight maintenance, as above, implies a general agreement as to its meaning. "Boresight", a word derived from ordnance usage relating gun bores to their aiming devices, is now widely applied to the relation of the optical axis of an optical system to some mechanical or functional reference axis (or axes).

Theoretically the optical axis of the optical system designed for objects at infinity can be defined in terms of the normal to a particular plane wave front. The reference wavefront has its source in a point at infinity, identified by the unique direction of all the normals to the 'particular' wavefront. One of these parallel 'normals' intersects the image of the reference point source at the focal point in the focal plane. This 'normal' or line is the optical axis of the system. In the ideal system, the diffraction pattern which constitutes the star image will be radially symmetrical about this intersection of the optical axis in the focal plane. Off-axis aberrations (e.g., coma) will be, dimensionally, some function of the radial distance from this focal point. In practice, it is this radial symmetry that is used to identify the optical axis.

The design and assembly of a 'pointing' optical system attempts to assure, as closely as possible, the coincidence of the optical axis with some functional axis of the instrument. A test for this coincidence is to physically rotate the unit about the optical axis with the on-axis star image in focus. Zero-deviation of the diffraction pattern at the focal point can be one of the simplest proofs of boresight maintenance (when the reliability of the mechanical axis of rotation can be simultaneously proved). For a description of some of the other classical methods of optical instrument alignments, see Ref. (60).

In the simplest case of the typical star tracker, the telescope axis will coincide as closely with the theoretical optical axis as the accuracy of fabrication and assembly permits (within a few thousandths of an inch).

Practically, then, 'the optical axis' is synonymous with 'the telescope axis'. The telescope axis may be functionally determined by the center of a precise field stop in the f. p., the null point (or possibly the peak) of some modulating device, light chopper, or field scanner in or near the focal plane.

In a typical Kollsman star tracking instrument, the telescope axis will intersect the trunnion (or elevation) axis at the same point that it intersects the vertical (or azimuth) axis. That they actually intersect at a single point is not important (except for the case of the tracker telescope whose first element is a fixed, concentric, spherical, dome-window). It is required that the optical axis be precisely orthogonal with the elevation axis (and, of course, the elevation axis orthogonal with the azimuth axis).

The original boresighting, in the simplest case of the typical astro-tracker, consists in establishing the above mentioned relationships, very precisely, with some mounting reference. This is performed with the tracker in an alignment and test stand which precisely simulates the normal celestial 'input'.

The five different techniques which are discussed below are used in the Kollsman instruments of which they are a part to serve a function related to boresight maintenance. They are selected to illustrate the practical accuracies which have been achieved, and to suggest the type of instrumentation from which may evolve those techniques capable of the higher order of accuracy required fore the spacecraft laser beam pointing boresight maintenance.

The first two of the techniques discussed are somewhat different versions of the type known as 'optical links'. The optical link is typically used to relate the pitch and roll of an instrument mount to a stable platform. The basis of this test is autocollimation.

The fourth illustration of Kollsman boresight maintenance techniques is one used to monitor the focus of a large space telescope. The method is unique and potentially capable of a high order of accuracy.

The last example is the method used in the same large space telescope to monitor what is called the telescope's 'fine guidance' (spacecraft pointing). A scanning technique senses the position of a star image with great accuracy.

1: The Optical Link of the Kollsman KS-134 Astrotracker System

The astrotracker of the KS-134 system was mounted directly above an inertial platform. The tracker includes pitch, roll, and azimuth gimbal systems slaved to the gyro platform by the optical link. The configuration is illustrated in Figure 18. Somewhat similar systems are described in Refs. (18), (61).

The gimbal and optical link arrangement establishes the vertical reference and true north for the astrotracker. Mounted on this azimuth gimbal is a relative bearing and elevation gimbal system for positioning the telescope. The telescope consists of the refractor-objective, accessory optics, scanner mechanism and sensor required to acquire and track.

The optical link was arranged as shown schematically in Figure 19. The collimating lens has an aperture of 1" D. and an effective focal length of 15". The illuminated aperture in the focal plane 15.07 in^2. A solid state sensor with an active area of 0.13"x0.05" on each of two opposite sides of each rectangular aperture detect plus and minus deviations of the autocollimated reference mirrors mounted on the inertial platform.

This optical arrangement although unsophisticated was reliable and exceeded the accuracy requirement of the astrotracker which it monitored, i.e. it had the capability to maintain these 3 axes of reference to better than 10 seconds of arc.

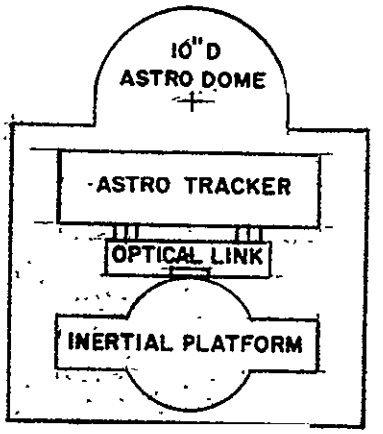

Figure 18. KS-134 Astro-Inertial System

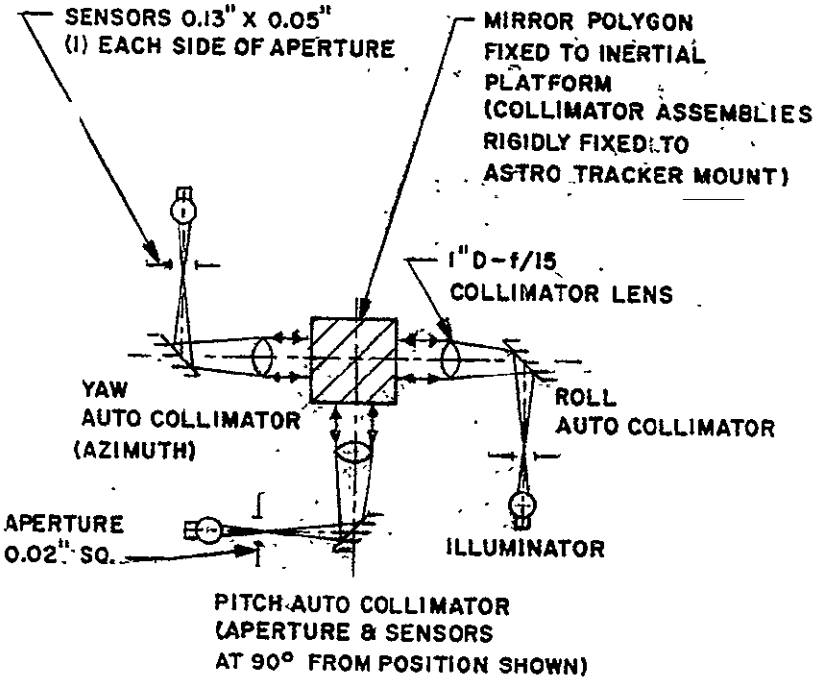

Figure 19. Optical Link Schematic

The one inch diameter aperture of the objective has a theoretical resolving power of only about 5 seconds of arc (the radius of the Airy disc). However, nulling optical devices of this type have demonstrated their reliability fore requirements of accuracy and sensitivity far in excess of their theoretical resolving power based on the Rayleigh criteria.

The relatively long focal length (15 inches) of the KS-134 optical link autocollimators was accommodated in the small package by simple folding with flat mirrors. The next similar system, accomplishes extreme compaction (optical miniaturization) in a much more sophisticated optical manner.

2. The Optical Link of the Kollsman KS-169 Astrotracker System

This optical link serves the same function as the one just described for the Kollsman KS-134 system. However, the optical system that serves as the autocollimator for this link has evolved to a much more sophisticated catadioptric optical design, than the earlier, simple, dioptric system.

The function and arrangement of the prism mirror reference mounted on the inertial platform and autocollimators mounted on the tracker relative bearing plate is almost identical with the KS-134 system, Refs. (18), (61).

In this system, similarly, modulated light is focused on a source reticle with a swuare aperture. The catadioptric optical system collimates the light, transmits it to the monitored, mirror-polygon reference, and then deflects the return beam to a detector reticle consisting of two square apertures. Balanced and oppositely polarized detector elements are placed behind these apertures. When the reflector is normal to the modulated, incident beam, the reflected beam strikes the detector reticle between the two apertures. Diffraction spillover at the edges results in equal and out-of-phase signals from the detector elements. These signals cancel and no resultant signal is applied to the amplifier.

If the mirror is deviated from normal to the optical axis, some unbalanced reflected light passes through one of the apertures. The direction of the deviation will determine which aperture receives excess illumination and the amplitude of the deviation, i.e., the amount of modulated excess illumination.

The autocollimating optical system of the KS-169 is a small package whose largest dimension is only one and one-half inches. Nevertheless, it has a resolution capability of 0.1 second of arc when used in a certain mode. It's long term null stability is better than 0.25 second of arc.

The significance of this advance in the evolution of an optical component with possible applicability to the problems of Boresight Maintenance is the possibility of small-fraction-of-a-second optical monitoring without the impractical, large aperture, long focal length systems which are conventionally prescribed.

3. The Apollo Optical System Autocollimating Test Feature

The Apollo Sextant-Telescope has a built in self-checking technique which is in a sense a boresight monitoring system. A schematic diagram of this system is shown in Figure 20, Refs. (23), (62).

The indexing mirror, which is at the space end of the sextant-telescope has a precise angular readout and although its normal, scanning, sextant function does not include the position where this mirror is at right angles to the optical axis, it can be so positioned by the astronaut for testing the alignment of the telescope and the sextant readout by autocollimation off this mirror.

Since it is a self-checking type device, the sensitivity and the accuracy of this test is that of the optical system itself.

It is offered as an example of boresight maintenance in recognition of the philosophy implied and also as an example of a visual, non-automatic function with possible applicability to boresight mainteance.

This Apollo system totally obscures one entrance pupil, but need not. Another version of this technique could sample a portion or zone of such an aperture.

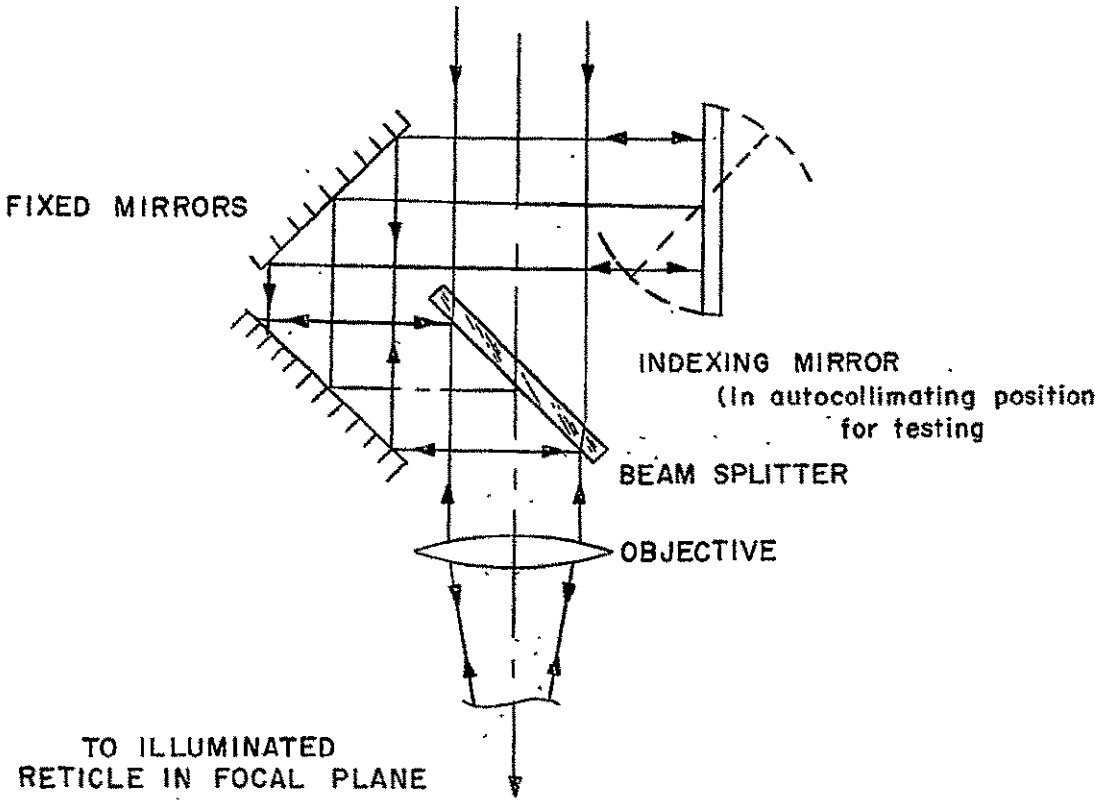

Figure 20. Diagram of the Apollo Telescope-Sextant Autocollimation Test

4. The Focus Detector of the Goddard Experiment Package

The function of this detector is to monitor the alignment of the experiment optical system. The detector uses the zero diffraction order energy from the spectrometer grating while the latter is fixed in the center of its scanning positions. To detect the magnitude and direction of the focus shift, light modulation on both sides of the normal focal plane is used, and the detected signals are telemetered to ground on two analog channels. Whenever a focus shift beyond the tolerance is detected, the experiment commands an appropriate repositioningof the secondary mirror until focusing is indicated by the detector signals, Refs. (16), (63).

The reflective optical system has a 0.0004 inch (10 μ) circle of confusion diameter in the focal plane. The corresponding diameter of the bundles at the planes of modulation is d_f = .020 inch (0.5 mm). For an assumed extreme focus shift of ± 0.100 inch from the nominal, the maximum light bundle diameter in either modulation plane is d max. = 0.040 inch (1.0 mm.).

The focus detector, shown schematically in Figure 23 makes use of a reed which vibrates in a plane perpendicular to the optical axis. (See Figure 22 Reed Assembly). The mirror surface is at 45° to the plane of vibration. By means of two mirrors located at particular positions on the reed corresponding to "L" and "S" (Fig. 21). The light rays are modulated before and after they pass thru the nominal focal plane F_2. The rays are then reflected to light sensors located in the respective light paths of the mirrors and the pulse width of the resulting signals are measured and compared. Equal pulse widths from both sensors indicate that the focus is correct.

If the pulse widths are unequal then their ratio indicates the magnitude and direction of the focus shift. In the present design, evaluation of the two signals is a function of ground equipment. Dependent upon the detected shift, correction commands are given by the experimenter.

The distance of the light sensors from the optical axis is kept to a minimum, thereby enabling the use of a small size light sensor, increasing the signal-to-noise ratio. However, this distance is large enough to prevent the reed from hitting the sensors.

According to preliminary calculations, the actual focusing error will be at least a factor of 2 smaller than the assumed range. Hence, an expected signal-to-noise above 10:1 can be counted on, when stars of first magnitude or brighter are used. An additional improvement in S/N will be obtained when checking the focus of stars with a low color temperature due to the sensor spectral response.

5. The Fine Guidance of the Goddard Experiment Package

The fine guidance subsystem of the Goddard Experiment Package has many of the elements of a typical boresight maintenance system. The system has demonstrated the capability of detecting star image position errors of the order of 0.1 second of arc, Refs. (16), (18), (63).

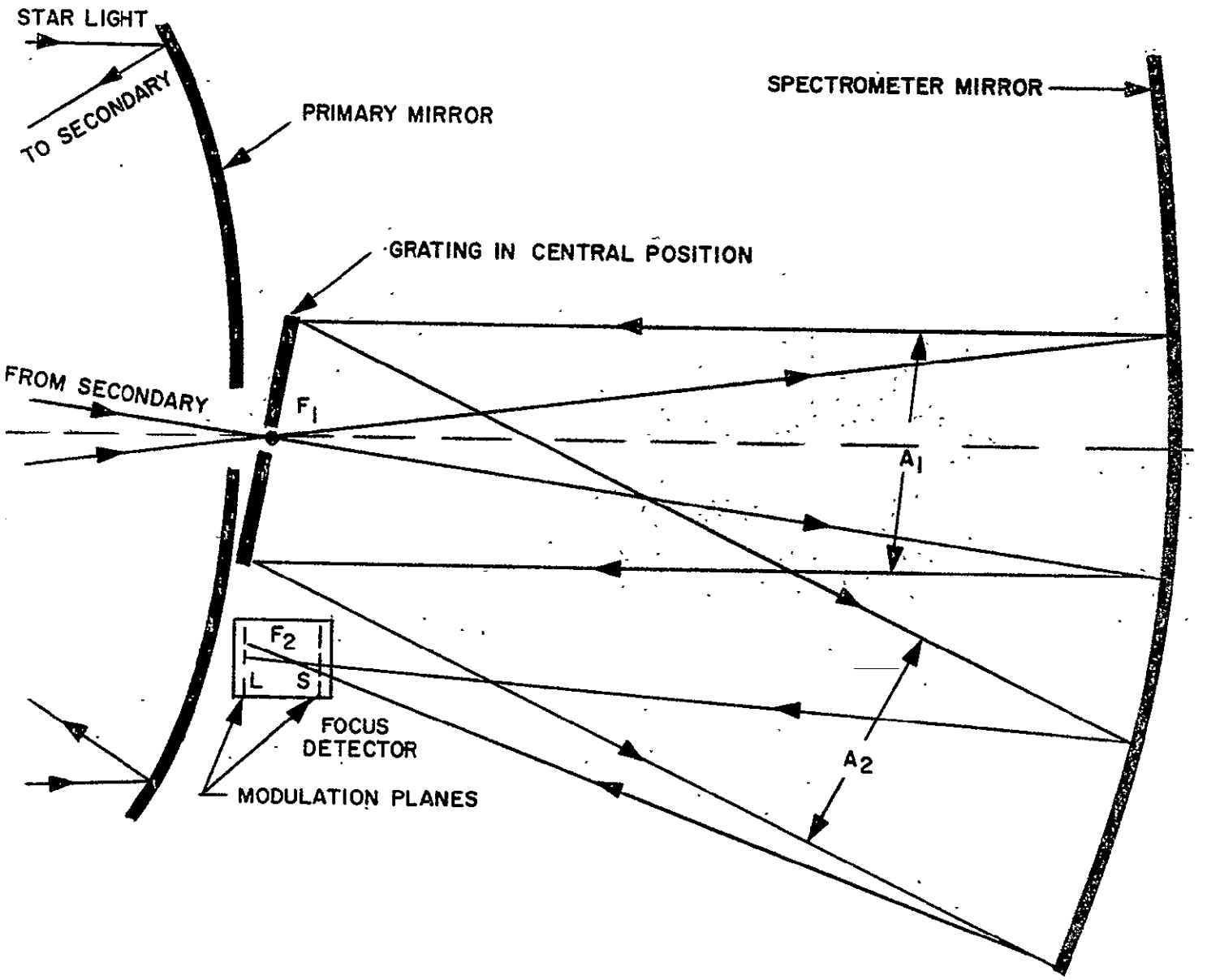

Figure 21. Optical Schematic of Focus Detector

(Zero Order Limit Rays)

Figure 21 shows an optical schematic of the GEP zero order limit rays for the control grating position. A star image is formed by the cassegrainian optics in F_1. Considering this image as a radiating point source, the spectrometer mirror collimated light bundle A_1 upon reflection from the grating, constitutes the zero-order light energy flux A_2. The GEP grating, blazed at 1200 A in the first order, has approximately 60% efficiency in the zero-order incident energy at the wavelengths from 0.4 to 1.1 micron (spectral response range of the solid state sensor).

The spectrometer mirror focuses the zero-order light energy A_2 in F_2. Due to the spectrometer mirror limitation (in diameter) only 70% of the incident energy A_2 is reflected.

Light modulating is performed by the detector scanner in two planes: S_1 for short focus detection and L for long focus detection as shown in Figure 22. Both are at a distance of 0.1 inch from the nominal focal plane, i.e., a focus shift detection range four times larger than the expected is here provided.

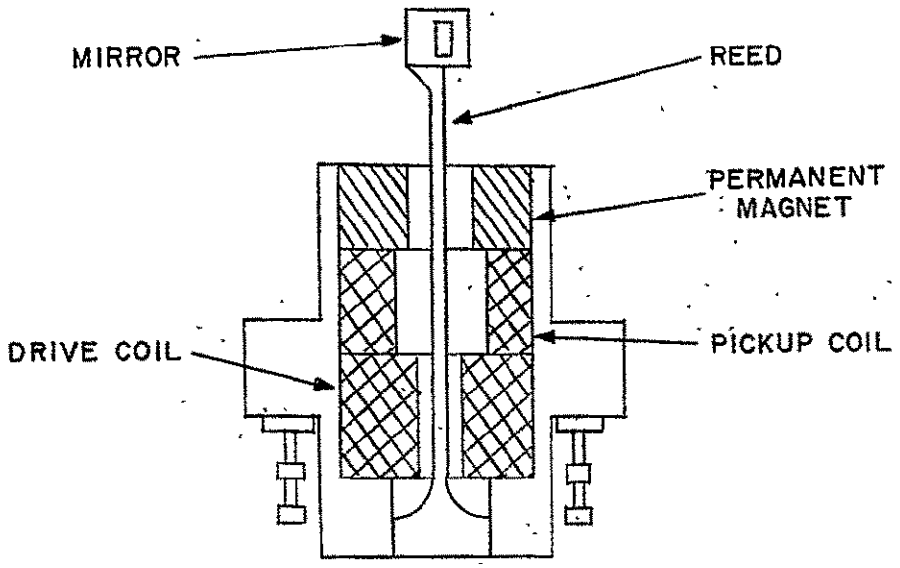

Figure 22. Optical Vibrating Reed Assembly

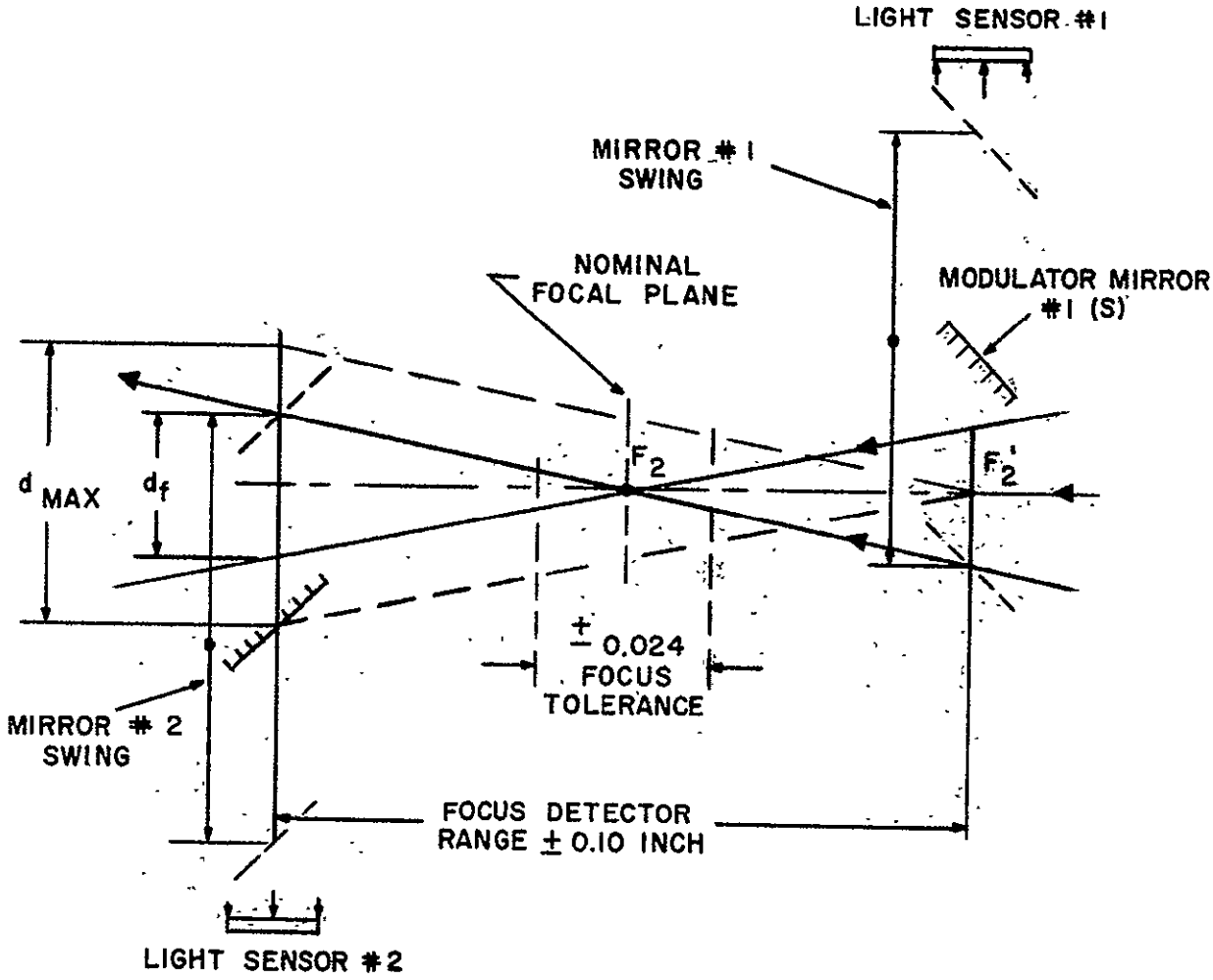

Figure 23. Focus Detector Functional Layout

(Goddard Experiment Package)

The fine guidance subsystem functions to give a star presence or acquisition signal which denotes that a star is present in its field of view and star position error signals in the pitch and yaw control axes. All three signals are used by the OAO stabilization and control subsystem in the spacecraft to correct the vehicle attitude in such a manner as to reduce the error in pointing towards the star. The system also provides a star magnitude signal which is compared with the command star magnitude. Referring to Figure 24, it is seen that the fine guidance pick-off mirror (within the aperture of the spectrometer mirror, rigidly mounted to it, and close to its vertex) taps off about 10% of the light of the light diverging from the entrance slot of the 38" D telescope's focal plane. This energy is reflected by the flat pick-off mirror (about 2 1/2" in diameter) to the aperture of a 5 1/4" D. Cassegrainian system of the Dall-Kirkham type designed for finite conjugates. The primary of this system is mildly aspheric (paraxial r = 19.4") and the 2" D convex secondary has an approximate radius of -15.7", giving an e. f. l. of 16.258" with a focal plane about 1.3" behind the vertex of the primary mirror.

This relay optical system is essentially diffraction limited over the required ±2 1/4 minutes of arc field.

In the focal plane of the Dall-Kirkham Cassegrain, there are a pair of reed scanners (similar to the vibrating reed shown in Fig. 22), one for each axis, which modulate the light passing through the focal plane to the photocathode of the photomultiplier tube.

The reed assembly consists of an aluminum base Ni-span reed, magnetic drive pick-off coil, and a permanent magnet. Ni-span was chosen as the reed material for its isoelastic properties with temperature.

This modulating reed has an aperture of 0.0354 x 0.0708 inches and the amplitude of its deflection is 0.050 inch giving an effective field stop of 0.0708 x .0708 inches, corresponding to a field of view of 4.5 x 4.5 minutes of arc.

The scanner amplitude stability is ±1% (max.) which is less than a half second of arc. Tests have demonstrated the device to be sensitive to star image deviations as small as 0.1 second of arc. The apportioned reliability factor (i.e. probability to operate in space for a duration of one year without suffering a catastrophic failure) is 0.9960.

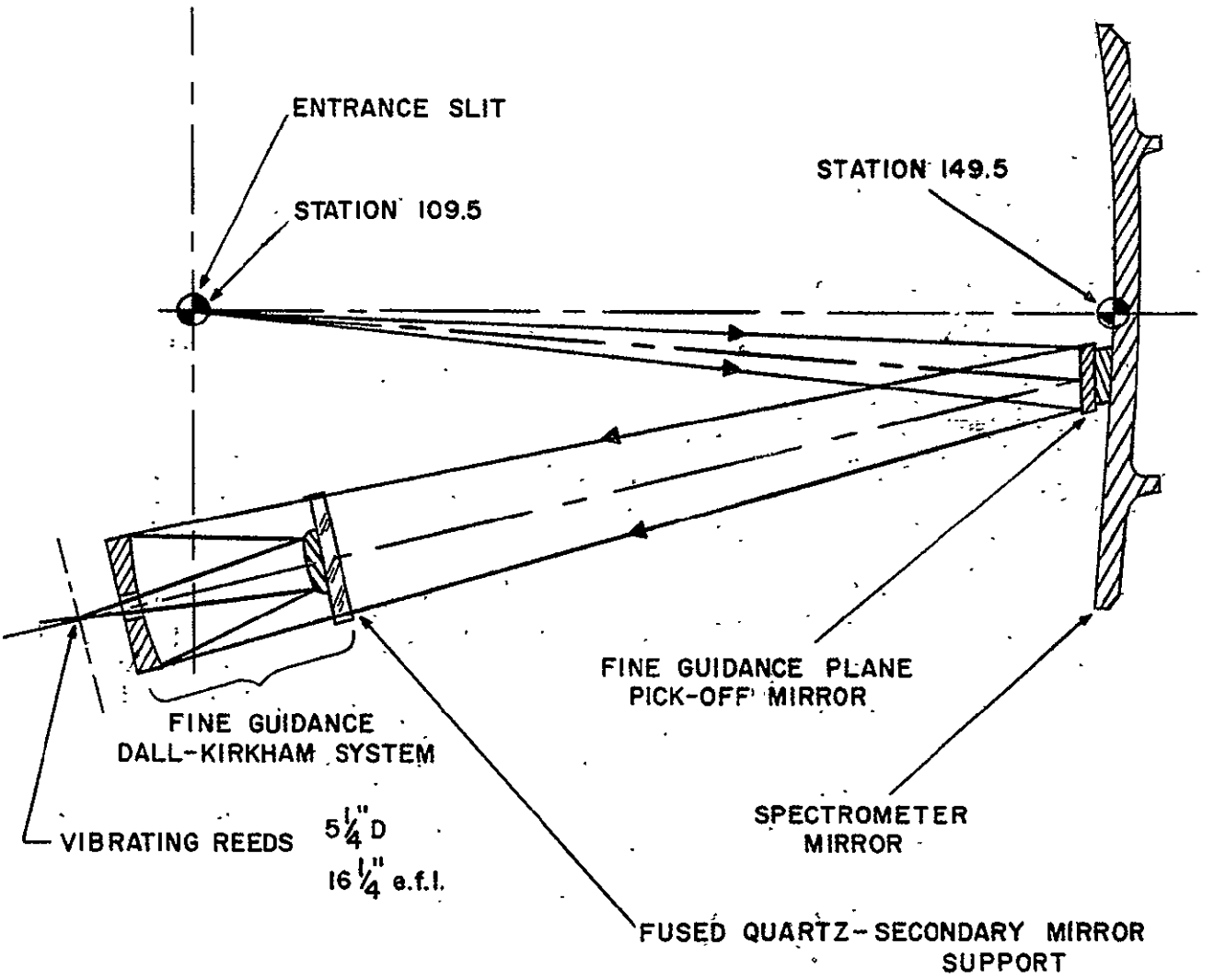

Figure 24. Fine Guidance Optical System for the Goddard Experiment Package

B. GENERAL CONSIDERATIONS ON OPTICAL ALIGNMENT

The techniques described in the previous section must be considered in the light of the discussion previously given in Section II E. The boresight maintenance depends on the configuration of optical measuring and positioning elements selected for steering relative to the reference axes provided in the hybrid open-closed cycle system, i.e., coarse and fine beam steering, phased arrays, etc. Although it is feasible to put a closed loop around the laser beam and the laser mount as described in Section II E, it may also be possible to include this stabilization feature in the beam measuring and positioning subsystem which is tied to the reference axes. This mode of operation is, of course, influenced by the internal and external spacecraft environment, Refs. (64), (65).

In other words, the more conventional mode is to sample the laser beam with a beam-splitter pick-off or a similar device to provide the input to the boresight maintenance subsystem. This input replaces the modulated star image in the 0.1 arc second accuracy techniques previously described, which are satisfactory for a one arc second beamwidth system. For the 0.1 and 0.01 arc second beamwidths, higher accuracies can be obtained with more sophisticated correlation techniques based on interferometry, Moire' fringes, or diffraction phenomena, Refs. (66), (67). In this mode, the absolute calibration of the fine beam steering subsystem must be independently guaranteed since it is strictly open-loop.

The other theoretically conceivable mode is to tie a closed loop from the laser beam directly to the reference axes. This mode is only desirable if it does not increase the accuracy requirements of these axes beyond the limits described in Section II E. If, however, at the same time, the closed loop can encompass the fine beam steering control, then some increase in the required accuracy may be worthwhile in the trade-off.

For the other end of the link, the techniques described in the preceding section can be utilized by the Earth station in larger, more rugged, and more precise configurations to provide accuracies similar to the more conventional astronomical techniques which are better than 0.1 arc second under slowly varying conditions, Refs. (68), (69). In addition, more sophisticated techniques based on interferometric or correlation techniques can be used to generate alignment accuracies of the order of 0.01 arc seconds. However, as described in Sections II E and II F,

the atmospheric problems associated with "In Vivo" operation add another dimension to the optical alignment problem for the Earth station, cf. the discussions in Section III. The problems associated with laser beam sampling and alignment will be analyzed in later reports.

VI. CONCLUSIONS

1. Deep space radio communications in the form of the NASA DSIF have successfully fulfilled all of the past and present NASA requirements for aerospace control and communications. However, future missions requiring high information rate, real-time data transmission transcend the performance capabilities of such systems.

2. An "In Vacuo" analysis of deep space laser communications exhibits significant potential for future missions. However, the performance under "In Vivo" conditions, which includes the effects of the atmosphere on the laser beams and interference due to extraneous sources of noise imposes additional constraints not only on the communications, but also on the pointing system.

3. A factor and variable analysis of the total complex including the space vehicle, the Earth station, and the environment has been prepared, exhibiting the factors, variables, errors and uncertainties which must be considered.

4. Although pure open and closed cycle systems are conceptually possible (that is, pure non-cooperative and cooperative systems), the factor and variable analysis indicates that a hybrid open-closed cycle combined system offers the best compromise between system complexity and component precision.

5. In the "In Vacuo" case, a bilateral symmetry exists on both ends of the communication links. In the "In Vivo" case, the link is strongly asymmetrical for very narrow beamwidths because of the Earth's atmosphere. For a conventional "lumped" system based on celestial tracking and monostatic radar philosophy, there are conflicting demands due to atmospheric random turbulence phenomena and extraneous noise. This trade-off points to the desirability of considering "distributed" systems similar to radio astronomical techniques and bistatic radar.

6. Preliminary analyses have been carried out on various aspects of laser beam propagation through the atmosphere such as absorption, angle of arrival fluctuations, intensity fluctuations, background radiation, and

optical heterodyne reception. Their magnitudes are too large to be neglected, i.e., the "In Vacuo" approximation. Actual systems must be designed for "In Vivo" operation.

7. Preliminary analyses have been conducted on various aspects of fine beam steering and boresight maintenance. Present-day techniques are suitable for a one arc second beamwidth system, but more sophisticated techniques will be required for the 0.1 and 0.01 arc second beamwidth systems.

VII. PROJECT ACTIVITIES FOR NEXT PERIOD

1. Project activities for the next period will follow the task sequence described in Section I, esp. Sect. I B, Figure 2. Because of delays and personnel changes, some taks originally scheduled for the first period have been postponed to the second and third periods.

2. In addition, emphasis will be placed on further atmospheric propagation analysis, in both directions of propagation, i.e., space-to-earth, earth-to-space. A trajectory will be prepared for a Mars fly-by mission to provide a numerical basis for systems analysis and preliminary error analysis. Part of the trajectory analysis will be devoted to the aberration and transit time compensations and implementation.

VIII. CONFERENCES

1. Fred Morrell, NASA Langley Research Center, Instrumentation Research Division, visited Kollsman on 17 August 1964 to discuss technical aspects of the beam pointing system with project personnel: A. Wallace, R. Arguello, J. Meader, G. Schuster, J. Eichenthal.

2. Messrs. R. F. Bohling, NASA Headquarters, and F. Morrell, NASA Langley, visited Kollsman on 17 and 18 September 1964 to review progress on the program. A presentation was made covering much of the systems material, Section II, and beam steering techniques, Section IV, by A. Wallace, Dr. S. Monaco, and R. Arguello.

IX. MANPOWER UTILIZATION

A. AUGUST-SEPTEMBER, 1964.

Project Director:	A. Wallace	- 256 hours
Project Engineer:	R. Arguello	- 160 hours

B. OCTOBER-NOVEMBER, 1964.

Project Director:	A. Wallace (1)	- 328 hours	
Project Engineer:	G. Strauss (1)	- 312 hours	(2)

Notes: (1) Full-time program participants.
(2) Assigned to program on October 5, 1964.

X. BIBLIOGRAPHY

(1) Space/Aeronautics, Vol. 41, No. 1, January, 1964. "Aerospace in Perspective" Issue, pp. 71-182.

(2) John W. Thatcher, "Deep Space Communication", pp. 54-63, Space/Aeronautics, Vol. 42, No. 1, July 1964.

(3) Space/Aeronautics, Technical Reference Series, Part 2, November, 1962, "Aerospace Electronics Advanced Communications", pp. 23-29, 35-48, 63-66.

(4) W. Huntley, Jr., "New Coherent Light Diffraction Techniques", pp. 114-122, I.E.E.E. Spectrum, Vol. 1, No. 1, January 1964.

(5) R. W. Terhune, "Nonlinear Optics", pp. 38-47, International Science and Technology, No. 32, August, 1964.

(6) E. B. Moss, "Some Aspects of the Pointing Problem for Optical Communication in Space", AIAA First Annual Meeting and Technical Display, Washington, D. C., 29 June- 2 July 1964.

(7) A. Wallace, "Proposal for Spacecraft Laser Beam Pointing System Study", Report No. KIC-RD 188, Kollsman Instrument Corporation, Elmhurst, N. Y., May 11, 1964

(8) A. Wallace, "Epistemological Foundations of Machine Intelligence", Nov. 11, 1963, Contract No. AF33(657)-9482, AF Report No. ASD-TDR-63-878.

(9) Contract No. NASW-929, National Aeronautics and Space Administration, NASA Headquarters, Washington, D. C. 20546, Title "Study of Laser Pointing Problems", Control No. 10-2878, dated August 10, 1964.

(10) NASA Request for Proposal No. 10-2878 dated April 15, 1964.

(11) F. Leary, "Television From Space", pp. 70-79, Space/Aeronautics, Vol. 41, No. 3, March, 1964.

(12) B. M. Oliver, "Some Potentialities of Optical Masers", pp.135-140, Proc. of the I.R.E., Vol. 50, No. 2, Feb., 1962.

(13) D. G. C. Luck, "Some Factors Affecting Applicability of Optical-Band Radio (Coherent Light) to Communication", pp. 359-409, RCA Review, Sept., 1961.

(14) G. K. Megla, "Some New Aspects for Laser Communications", pp. 311-315, Applied Optics, Vol. 2, No. 3, March, 1963.

(15) K. L. Brinkman, W. K. Pratt, E. J. Vourgourakis, "Design Analysis For a Deep Space Laser Communications System", pp. 35-46, Microwaves, Vol. 3, No. 4, April, 1964.

(16) H. B. Hallock, "Optics in the Orbiting Astronomical Observatory", pp. 155-163. Applied Optics. Vol. 1. No. 2, March, 1962.

(17) S. Moskowitz, P. Weinschel, "Instrumentation for Space Navigation", pp. 289-306, I.E.E.E. Transactions on Aerospace and Navigational Electronics, Vol. ANE-10, No. 3, Sept. 1963.

(18) J. Zuckerbraun, "High Reliability Scanners for Stellar Navigation", Electronics, May 11, 1962.

(19) M. Meisels, "Laser Phased Arrays Ready for Breadboarding", pp. 6-9, Microwaves, Vol. 3, No. 3, March 1964.

(20) L. Zadeh, "From Circuit Theory to Systems Theory", pp. 856-865, Proc. I.R.E., Vol. 50, No. 5, May, 1962.

(21) See Ref. (3), J. Holahan, pp. 6-17.

(22) F. V. McCanless, "A Systems Approach to Star Trackers", pp. 182-193, I.E.E.E. Transactions on Aerospace and Navigational Electronics, Vol. ANE-10, No. 3, Sept. 1963.

(23) S. Moskowitz, P. Weinschel, "Instrumentation for Space Navigation", pp. 289-306, same issue as Ref. (22).

(24) A. M. Naqvi, R. J. Levy, "Some Astronomical and Geophysical Considerations for Space Navigation", pp. 154-170, same issue as Ref. (22).

(25) B. O. Koopman, "Theory of Search", Part I, "Kinematic Bases", J.O.R.S.A., pp. 324-346, Vol. 4, 1956; Part II, "Target Detection", J.O.R.S.A., pp. 503-531, Vol. 4, 1956; Part III, "Optimum Distribution of Searching Effort", J.O.R.S.A., pp 613, etc., J.O.R.S.A., Vol. 5, 1957.

(26) E. Posner, "Optimal Search Procedures", pp. 157-160, I.E.E.E., PGIT, Vol. IT-9. No. 3, July, 1963.

(27) J. S. Greenberg, "On the Narrow Beam Communication System Acquisition Problem", I.E.E.E. Trans. on Military Electronics, Jan., 1964.

(28) R. Carpenter, "Comparison of AM and FM Reticle Systems", pp. 229-236, Applied Optics, Vol. 2, No. 3, March, 1963.

(29) J. Abate, "Star Tracking and Scanning Systems, Their Performance and Parametric Design", pp. 171-181, same issue as Ref. (22).

(30) Povesjil, Raven, Waterman, "Airborne Radar", Van Nostrand, Princeton, N. J., 1961.

(31) J. A. Fusca, "Laser Communications", pp. 58-77, Space/Aeronautics, Vol. 41, No. 5, May, 1964.

(32) K. M. Siegel, "Bistatic Radars and Forward Scattering", pp. 286-290, National Aeronautical Electronics Conference Proceedings, Dayton, Ohio, I.R.E., PGANE, May 12-14, 1958.

(33) Proceedings of the I. R. E., "Scatter Propagation Issue", Vol. 43, No. 10, October 1955.

(34) J. D. Kraus, "Recent Advances in Radio Astronomy", pp. 78-95, I.E.E.E. Spectrum, Vol. 1, No. 9, September, 1964.

(35) R. W. Bickmore, "Adaptive Antenna Arrays", pp. 78-88, I.E.E.E. Spectrum, Vol. 1. No. 8, August, 1964.

(36) L. J. Cutrona, "Optical Computing Techniques", pp. 101-108, I.E.E.E. Spectrum, Vol. 1, No. 10, October, 1964.

(37) F. Harary, "Graph Theory and Electric Networks", pp. 95-109, I.R.E. Transactions on Information Theory, Vol. IT-5, May, 1959.

(38) P. Bello, "Time Frequency Duality", pp. 18-33, I.E.E.E. Transactions on Information Theory, Vol. IT-10, No. 1, Jan. 1964.

(39) J. S. Frame, H. E. Koenig, "Matrix Functions and Applications - Part III", pp. 100-109, I.E.E.E. Spectrum, Vol. 1, No. 5, May 1964.

(40) "Study and Investigation of Acquisition and Tracking of Optical Communications", Technical Documentary Report No. ASD-TDR-62-733, Philco Corporation Scientific Laboratory, Blue Bell, Pa., Contract No. AF33(616)-8392, ASTIA No, AD-293452, November, 1962.

(41) Tatarski, V.I., "Wave Propagation in a Turbulent Medium". (McGraw-Hill Book Company, Inc., New York 1961).

(42) Chermov, L. A., "Wave Propagation in a Random Medium" (McGraw-Hill Book Company, Inc., New York 1961).

(43) Goodwin, F.E., "Laser Propagation in the Terrestrial Atmosphere", Paper presented at the First Conference on Laser Technology, San Diego, Calif.; Nov. 12-14.

(44) Ligda, M., "Meteorological Observations with LIDAR", Stanford Research Institute, Menlo Park, California, Paper Presented at the First Conference on Laser Technology, San Diego, California, Nov. 12-14.

(45) Elterman, L. "A Series of Stratospheric Temperature Profiles Obtained with the Searchlight Technique", J. of Geo. Res., 58:4, Dec. 1953.

(46) Long, R. K., "Atmospheric Attenuation of Ruby Lasers", Proc. I.E.E.E., p. 859-860, May 1963.

(47) Allen, C. W., "Astrophysical Quantities". University of London, 1957.

(48) NASA Report CR-55812, "Study on Optical Communications From Deep Space", Interim Progress Report, Hughes Aircraft Company, Culver City, California, 27 March 1963 through 11 May 1963.

(49) "Handbook of Geophysics for Air Force Designers", Geophys. Res. Dir. AFCRC, ARDC, USAF, 1st Ed., 1957.

(50) KIC Internal Report, "General Model of Electro-Optical Systems", 1961, Section 6.

(51) Hufnagel, R. E., "Understanding the Physics of Seeing through Turbulent Atmospheres", Abstracted from Advanced Range Instrumentation Presentation made by Perkin-Elmer Corporation at Patrick AFB, Fla., Nov. 20, 1963.

(52) Hufnagel, R. E. and Stanley, N. R., "Modulation Transfer Function Associated with Image Transmission through Turbulent Media", J. Opt. Soc. Am. 54, 52 (1964).

(53) Hosfeld, R., "Measurements of the Size of Stellar Images", AFCRC -TN-55-873, Joint Scientific Report 2 (June 1955).

(54) NASA Report CR-53466, "Optical Space Communications System Study", Final Report, Vol. III, System Topics Part II, Spacecraft Department, Missile and Space Division, General Electric Company, Valley Forge Space Technology Center, Philadelphia, Pa., Feb. 1964.

(55) Gardner, S., "Some Effects of Atmospheric Turbulence on Optical Heterodyne Communications", Presented at 1964 I.E.E.E. International Convention.

(56) Fried, D. L. and Cloud, J. D., "Theoretical Examination of the Effect of Atmospheric Turbulence on Optical Propagation", Technical Memorandum No. 94, A Paper Presented at the 1964 Spring Meeting of the Optical Society of America, Washington, D. C., April 3, 1964.

(57) Gröbner, W. and Hofreiter, N., "Integraltafel, Bestimmte Integrale", p. 198, No. 5.

(58) Coherent Optical Beam Steering Techniques. Report No. RADC-TDR-63-450, Vol. I & II - Jan. 1964.

(59) Technical Note on Heterodyne Detection in Optical Communication. TRG-168-TDR-1, 30 Nov. 1962.

(60) B. K. Johnson, "Optics and Optical Instruments", Chapters IV, V, VIII, Dover Publications, New York, 1960.

(61) J. Greene, "The Celestial Tracker as an Astro Compass", pp. 221-235, same issue as Ref. (22).

(62) "Apollo Optical Unit Assembly-Sextant Self-Collimator Test", Document JDC 02061 FTM 1011000, Kollsman Instrument Corporation, Elmhurst, New York, Contract NAS9-499.

(63) Goddard Experiment Package of OAO Reports, Kollsman Instrument Corporation, Elmhurst, New York, Contract NAS5-1752.

(64) Lyman Spitzer, Jr., "Space Telescopes and Components", pp. 242-263, The Astronomical Journal, Vol. 65, No. 5, June, 1960.

(65) "Mariner Mission to Venus", by the Staff, Jet Propulsion Laboratory, McGraw-Hill Book Co., N. Y., 1963.

(66) Emile Wolf, Progress In Optics, Vol. II, pp. 45-57, 75-107. Pub. John Wiley & Sons, Inc., 1963.

(67) J. Guild, The Interference Systems of Crossed Diffraction Gratings. Pub. Oxford at the Clarendon Press, 1956.

(68) Peter van de Kamp, "Problems of Long-Focus Photographic Astronomy", pp. 9-15, Applied Optics, Vol. 2, No. 1, January, 1963.

(69) H. Eichhorn, "The Relationship Between Standard Coordinates of Stars and the Measured Coordinates of their Images," pp. 17-21, Applied Optics, Vol. 2, No. 1, January, 1963.

AERO/SPACE RESEARCH AND DEVELOPMENT

SYSTEMS MANAGEMENT

SPACECRAFT COMPONENTS AND SYSTEMS

ASTRO TRACKERS

AUTOMATIC ASTRO COMPASSES

DISPLAY SYSTEMS

ORDNANCE

ELECTROMECHANICAL SYSTEMS

SIMULATORS

OPTICAL ELECTRONICS

MISSILE COMPONENTS AND SYSTEMS

JET ENGINE INSTRUMENTS

FLIGHT INSTRUMENTS

INTEGRATED FLIGHT INSTRUMENT SYSTEM

OPTICAL SYSTEMS AND COMPONENTS

DOPPLER COMPUTATION SYSTEMS

PERISCOPIC, HANDHELD AND PHOTOELECTRIC SEXTANTS

FLIGHT SIMULATOR INSTRUMENTS

LABORATORY TEST INSTRUMENTS

UNDERSEA WARFARE SYSTEMS

GROUND SUPPORT EQUIPMENT

Kollsman Instrument Corporation
SUBSIDIARY OF STANDARD KOLLSMAN INDUSTRIES, INC

80-08 45th AVENUE, ELMHURST, N. Y. 11373